

Chapter 1

Introduction

The notion that plastics could conduct electricity never came to the attention of scientists until their accidental discovery in 1977. These special plastics called conducting polymers have attracted a lot of attention in the research and scientific community because of their possible and promising applications. The combination of their polymeric nature and electronic conductivity put them in a favorable position which conventional inorganic materials are not in with regard to applications and products. Conducting polymers offer new applications in areas such as molecular electronics, electronic drug delivery, large screen displays and tunable electromagnetic interference shielding to state a few.

Despite their profound application possibilities charge transfer is still not very well understood. In this study we investigate charge transfer properties of conducting polymers in the temperature range 30 – 450 K.

Semiconductor current-voltage characteristics of the material are observed below 300 K. The effect of annealing on the current-voltage properties of the polymer is also studied at temperatures between 300 K and 450 K. Fourier transform infra-red (FTIR) spectroscopy was used in relating conductivity changes to the molecular structure of the polymer. Thermal analysis was also applied in relating conductivity changes to possible loss of substances from the polymer as a result of annealing.

Chapter 2 gives an overview of the properties of the family of conducting polymers.

In the present study, all the experimental work was done on a conducting polymer called polyaniline. Chapter 3 details the properties of polyaniline. Polyaniline was chosen

because of its easy synthesis, low cost of synthesis and stability when compared to other conducting polymers.

A number of factors contribute to the overall measured conductivity of conducting polymers. In chapter 4 charge transfer in conducting polymers is analyzed in terms of the conductivity determining factors.

In chapter 5, methods applied in the characterization of polyaniline are detailed. Chapter 6 gives some of the technological applications of conducting polymers. A full description of experimental techniques used in the present study is given in chapter 7. Chapter 8 gives the experimental results for the charge transfer study between 30 K and 450 K.

In Chapter 9 the discussion to the results obtained is given. Chapter 10 includes a conclusion to this study and suggestions for further reading.

Chapter 2

Overview of Conducting Polymers

The aim of this chapter is to describe conducting polymers (CPs) in a simplified but complete way. CPs are described here based on the approach used for the inorganic semiconductors. It is encouraging to note that this approach is reasonably successful, as evidenced by our results. The study of CPs is “relatively” new, the literature base, although rapidly expanding, is still relatively small. Most of the literature used in this chapter and the proceeding chapters are works of the pioneers and highly acclaimed researchers in this field, notably: distinguished Ohio State University Professor A. J Epstein, A. G. MacDiarmid at Pennsylvania University, J.A Heeger, B. Wessling from Ormecom Pvt. limited, M. Gosh, B. Friend, J. Bredas, S. Sethi, J. Tsukamoto, M. Conwell. R. Menon and many others.

Models from condensed matter (solid-state) physics for the treatment of semiconductors are the closest for arriving at a generalized understanding of conducting polymers, and thus have been adopted in broad measure by workers in the conducting polymer field¹. The band structure description of CPs was first lucidly presented by J. Bredas *et al*² on polypyrrole. Quantum chemistry and the Su-Schireffer-Heeger (SSH) Hamiltonian and its variants have been widely used to study the electronic structure of CPs and for successfully describing the ground state of such systems^{2,3}. For more information on the theoretical study of CPs, the reader is referred to references marked with an “*” at the end of this chapter.

2.1 The background of conducting polymers

The interest in CPs began in 1977, after Heeger/MacDiarmid and the Shirakawa group discovered that polyacetylene exposed to iodine vapors develops very high and well-

characterized conductivities. However, as early as 1862 Letheby⁴ reported chemical oxidative polymerization of aniline (a building unit for polyaniline (Pan)). At the beginning of the 20th century, Mecoy and Moore⁴ suggested electrical conductivity in organic solids but nobody took cognisance of it for the reason that polymers were believed not able to conduct electricity⁴. Since 1957, studies of electrochemical oxidation of aromatic monomers, now widely used as one method of synthesis of CPs, have been reported under various descriptions such as “electro-organic preparations” and “electro-oxidations”. As early as 1968 dall’Ollio⁴ described electropolymerization of polypyrrole. From this and the above information, the discovery of CPs in 1977 was in actual fact a rediscovery of CPs⁴.

After the discovery of conducting polyacetylene in 1977, the 1979 discovery of electrochemical doping of polyphenylene vinylene (PPV) opened many doors to the study of CPs⁵. Several CPs and their derivatives have been discovered since then. Another important feature of electrochemical processing has been the ability to study the doping process using the voltametry method⁶.

The field of CPs is one of the most rapidly growing research fields from both a fundamental as well as a technological point of view, this is evidenced by the involvement of big companies such as Philips (Netherlands), Zipperling (Germany) (through its subsidiary Ormecon), as well as NASA (through its activity in sponsoring research) and a sizeable number of top international universities. Further evidence of how active research in CPs is, is the number of websites and patents currently registered. By 1986 the first polymeric device, a button cell, was produced by Seiko. Unfortunately the device failed to make an appreciable market impact. At present, several commercial conducting polymer (CP) based products are available on the market⁷.

Despite the commercialization of CP based products, charge transfer phenomena in CPs is still not well understood. The present commercialization is based on consistence in the electronic characteristics of the material, synthesis conditions and improved properties

such as morphology and crystallinity. In our present study, we attempt to contribute towards the understanding of the charge transfer characteristics of CPs.

2.2 The Conducting Polymers

CPs are plastics made out of small building blocks called monomers just like ordinary plastics. In addition to displaying the well known properties of plastics, CPs can display special properties such as electrical conductivity, electroluminescence, photoconductivity and lasing which ordinary plastics do not. Figure 2.1 shows the monomeric units of some of the well-studied CPs.

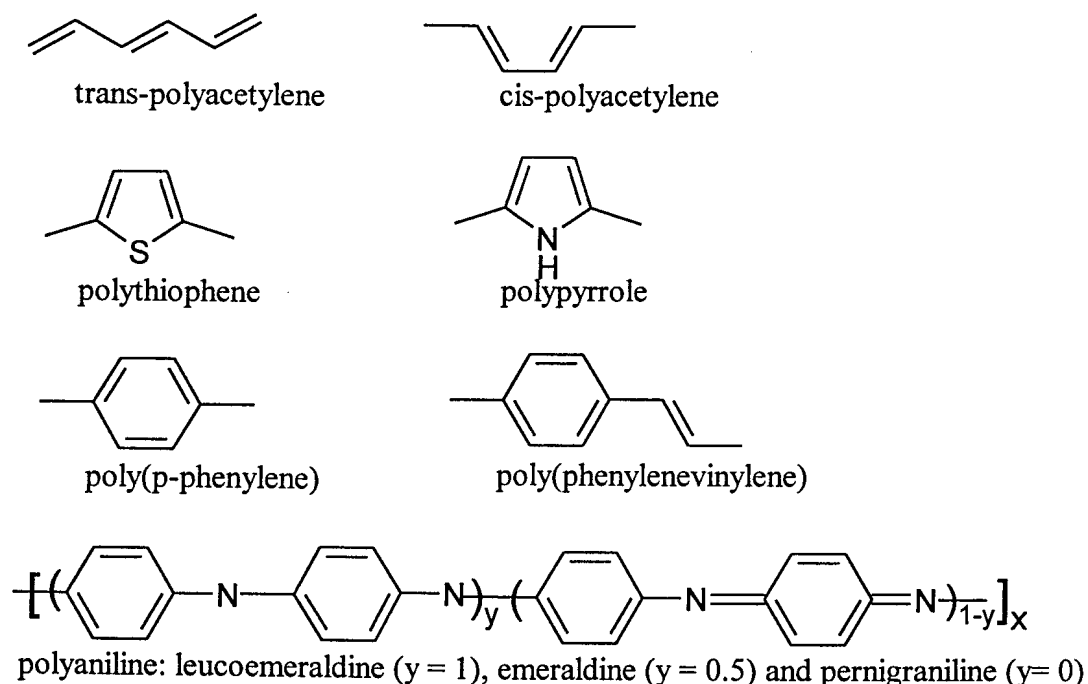


Fig (2.1): The monomers of some of the well studied CPs. Polyaniline is shown in its three possible oxidative states⁸.

A common feature of CPs is the alternation of single and double bonds, at least in the backbone of the polymer structure⁹. CPs are characterized by a delocalized π -electron system along the polymer backbone. The delocalized π -electron system, figure 2.2,

confers semiconducting properties to the polymer and gives it the ability to support positive and negative charge carriers with high mobility along the polymer chain¹⁰.

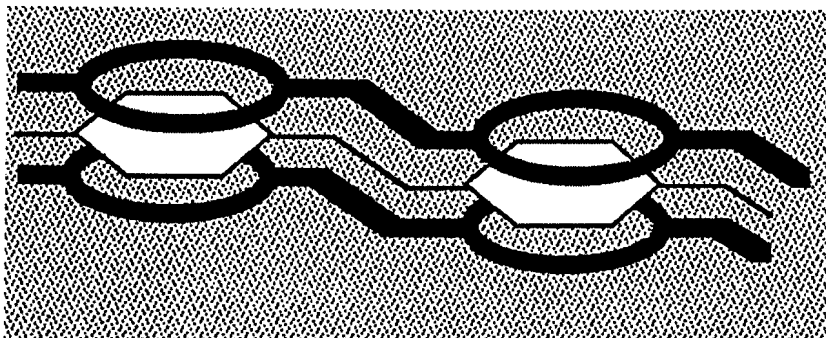


Fig (2.2): Overlap of the p-orbitals results in a delocalized π -electron cloud¹⁰.

2.3 Attractive properties of CPs

- i. They have many of the advantages of conventional inorganic semiconductors including the formation of Schottky and ohmic contacts with metals^{11, 12}.
- ii. For application in electronics, the electronic properties are locked into the molecular structure instead of being produced by the fabrication or processing technique. This unique feature ensures a suitable control of the electronic/optical properties of a resulting device by altering/modifying the organic molecular structure before fabricating the actual device.
- iii. The degree of conductivity is readily adjusted by controlling the structural order of the material and through the process of doping¹³.
- iv. CPs are easier to synthesize than inorganic materials, for example, compare epitaxial growth of silicon to the spinning of polymer thin films.
- v. CPs display a wide variety of properties, ensuring a vast number of potential applications in a large number of technologies¹⁴.
- vi. They offer novel applications such as artificial muscles⁴, electrochemical drug-delivery⁶, electrochromic windows and displays¹⁵, polymer based rechargeable batteries¹⁶, flexible light emitting diodes¹⁷, polymer based anticorrosion coatings^{6,18}, and many other applications.

- vii. They stand to substitute metals and other materials in applications such as, electromagnetic interference shielding^{14, 8}, where they have the advantage of lightweight and a tunable electronic shielding efficiency¹⁴.

2.4 Bonding and the semiconductor nature

To gain an understanding of the nature of CPs, we have to shed light on the structure and electrical properties of these materials. The extent of delocalization of π -electrons along the polymer backbone and the extent of interchain delocalization plays a dominant role in the electrical and optical properties of polyconjugated systems¹⁹.

Consider the s and p orbitals of an atom. The s orbitals are spherical and p orbitals are dumbbell shaped and are oriented at 90° to each other as depicted in figure 2.3.

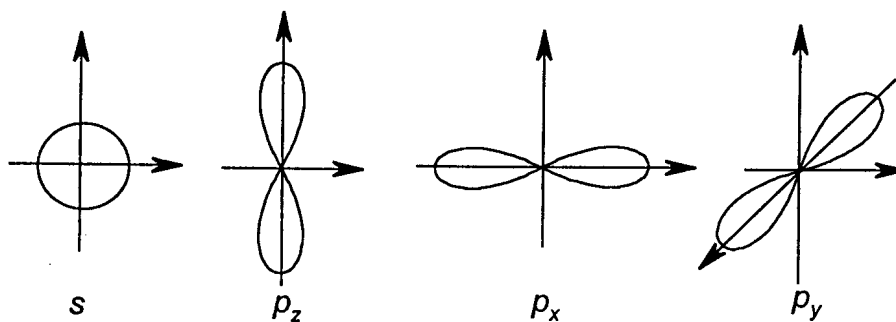


Fig (2.3): Orbital shapes for s and p_z , p_x and p_y orbitals respectively²⁰.

In a polymer molecule, bonding involves the p as well as the s orbitals of the atoms. The mixing of these atomic orbitals results in the chemical bonds in polymers. A covalent bond formed from end-to-end overlap of the atomic orbitals give σ bonds, while side-ways overlap of the p -orbitals gives π -orbitals. Figure 2.4 depicts the molecular orbitals formed from the overlap of p orbitals²⁰.

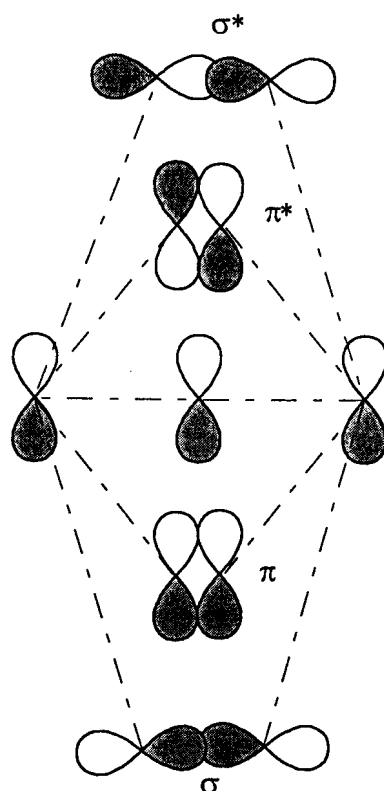


Fig (2.4): The overlap of p-orbitals to give bonding (σ and π) and antibonding (π^ and σ^*) molecular orbitals.*

The atomic orbitals that are not available for bonding will hold lone pairs. The remainder of the orbitals will overlap with each other to form σ bonds (head to head overlap) or π - bond (sideways overlap). π bonds may cover more than two nuclei and are characterized by the increased electron density above and below the imaginary line connecting the two nuclei²⁰.

When describing bonding in organic substances in terms of the molecular orbital theory, we use the postulate that molecular orbitals are a linear combination of atomic orbitals LCAO²⁰.

If φ_A and φ_B are the interacting atomic orbitals for atoms A and B respectively, a linear combination of the two atomic orbitals will produce two molecular orbitals φ_{MOI} and φ_{MOII} :

$$\varphi_{MOI} = a\varphi_A + b\varphi_B$$

$$\varphi_{MOII} = c\varphi_A - d\varphi_B$$

In terms of electron density, *MOI* gives a high concentration of electron charge between nuclei and is called the bonding (π) molecular orbital. *MOII* gives a lesser concentration and is called the anti-bonding (π^*) molecular orbital²⁰, as illustrated in figures (2.4 and 2.5) for the case of diatomic molecules. As the atoms are brought together, the *s* orbitals can overlap, forming σ_s and σ_s^* molecular orbitals; the p_x orbitals also overlap, forming another set of σ molecular orbitals of different energy, σp_x and σp_x^* . The p_y and p_z orbitals, overlap side to side and form a different set of molecular orbitals known as the $\pi p_y/\pi p_z$ and $\pi p_y^*/\pi p_z^*$ respectively (figure 2.4). The energies of the molecular orbitals and their relation to the atomic orbitals from which they came are shown in figure 2.5. The bonding molecular orbitals have lower energies than the atomic orbitals p_y and p_z from which they came. Note that the atomic orbitals p_y and p_z have the same energies²⁰.

The energy order of molecular orbitals is as follows: σ -type orbitals (the lowest in energy), π -type orbitals (non-bonding type of orbitals such as lone pairs), π^* -type orbitals and σ^* -type orbitals being the highest in energy. Each molecular orbital has a characteristic energy. Electrons occupy these orbitals according to the Pauli exclusion principle; electrons fill the lowest energy levels first. Orbitals of the same energy will be occupied by one electron each before a second electron is added to any one of the equal-energy orbitals²⁰.

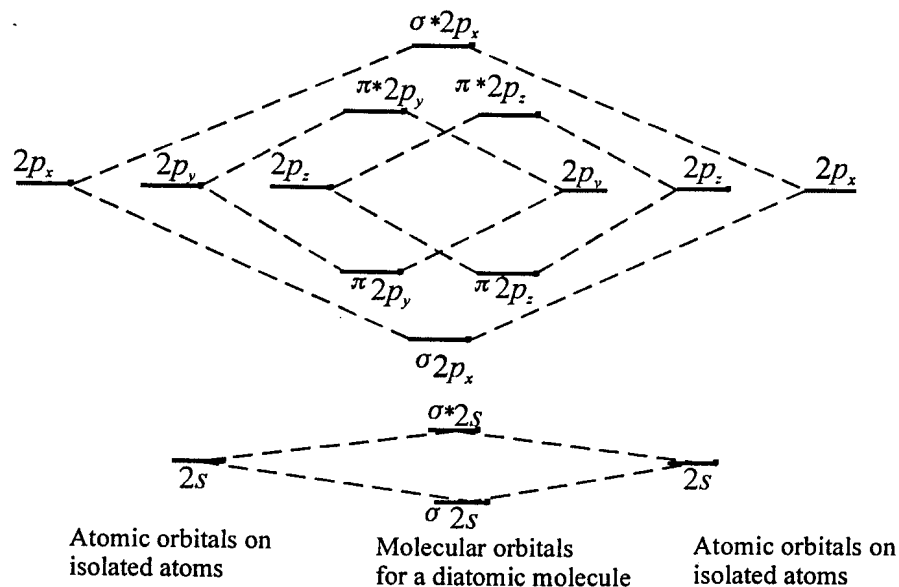


Fig (2.5): Atomic and molecular energy levels in a diatomic molecule, illustrating the concept of, σ/σ^ and π/π^* -orbitals²⁰.*

The overlap of molecular electronic states produces bands. The overlap of the extended π -bands or lone pairs (non-bonding electrons) becomes the valence band called HOMO (highest occupied molecular orbital) and the overlap of the π^* -bands becomes the conduction band LUMO (lowest unoccupied molecular orbital); if there is no π system empty σ^* orbitals form the LUMO band. The density of states – that is, the number of energy levels per eV between the top of the π orbitals (valence band) and the bottom of the π anti-bonding (π^*) orbitals (conduction band) – is zero within the bandgap (E_g). Hence when electrons are removed from the pristine (undoped) CP, they will be removed in a significant amount only from the top of the valence band. Figure 2.6 illustrates the density of states in a CP in terms of π and π^* molecular orbitals.

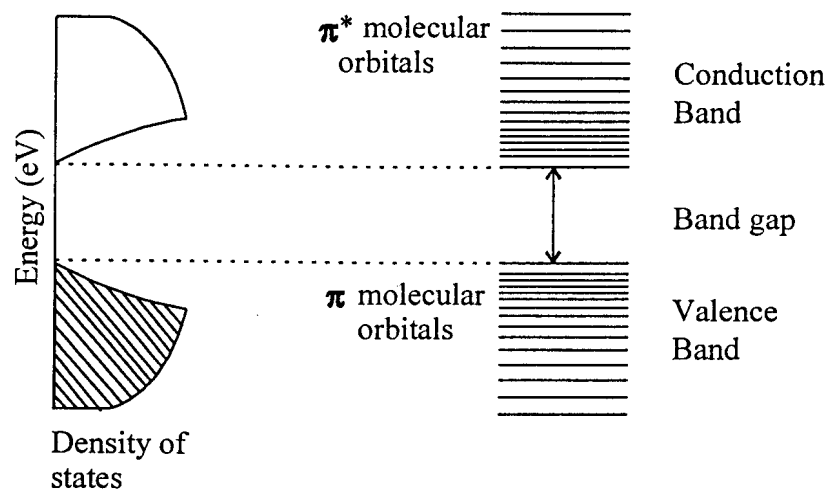


Figure (2.6): The left part of the diagram is the conventional density of states diagram for CP. The right part of the diagram depicts this in terms of π and π^ molecular orbitals.*

2.5 Conductivity classification

The electrical conductivity of CPs varies widely depending on a number of factors such as synthesis conditions, dopant used and the doping level. Based on these factors, CPs can be classified into the following groups: conductors (metals), semiconductors and insulators. Figure 2.7, depicts typical bandgaps of the 3 classes of materials in terms of LUMO and HOMO bands²¹.

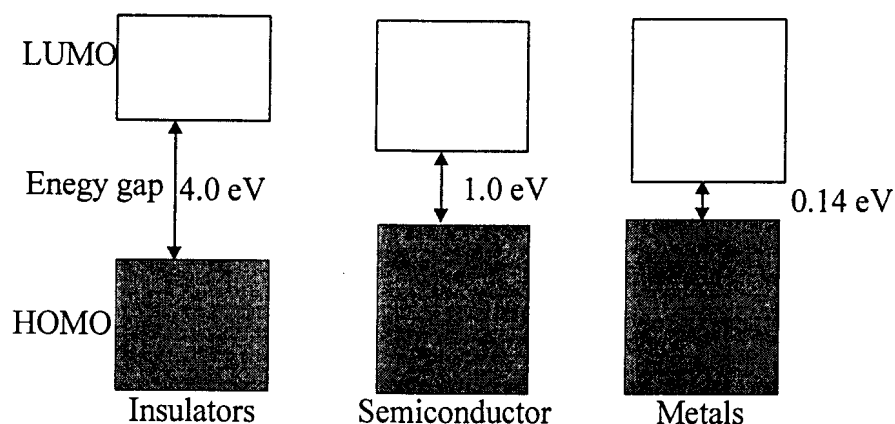


Fig (2.7): The three classes of conductivity (insulators, semiconductors and metals) are given in terms of typical energy bandgaps²¹.

The range of conductivities of the different classes of materials is shown in Figure 2.8, and from this it can be readily appreciated that, in order to render a conventional polymer conductive, its electrical conductivity should be increased by several orders of magnitude²². Since the conductivity of CPs can be adjusted through the process of doping, attaining different conductivity levels widens the scope of applications. Thus a single CP can have insulating, semiconducting and metallic conductivities, depending on the application for which the CP based device is designed to perform, polyacetylene⁵, as an example can have a conductivity range from 10^{-6} to almost 10^6 S/cm. Such applications include gas sensors, humidity sensors, temperature controllers and adjustable electromagnetic interference shielding, to state a few. The principle of operation is based on the change in conductivity as a function of the change in conditions being measured.

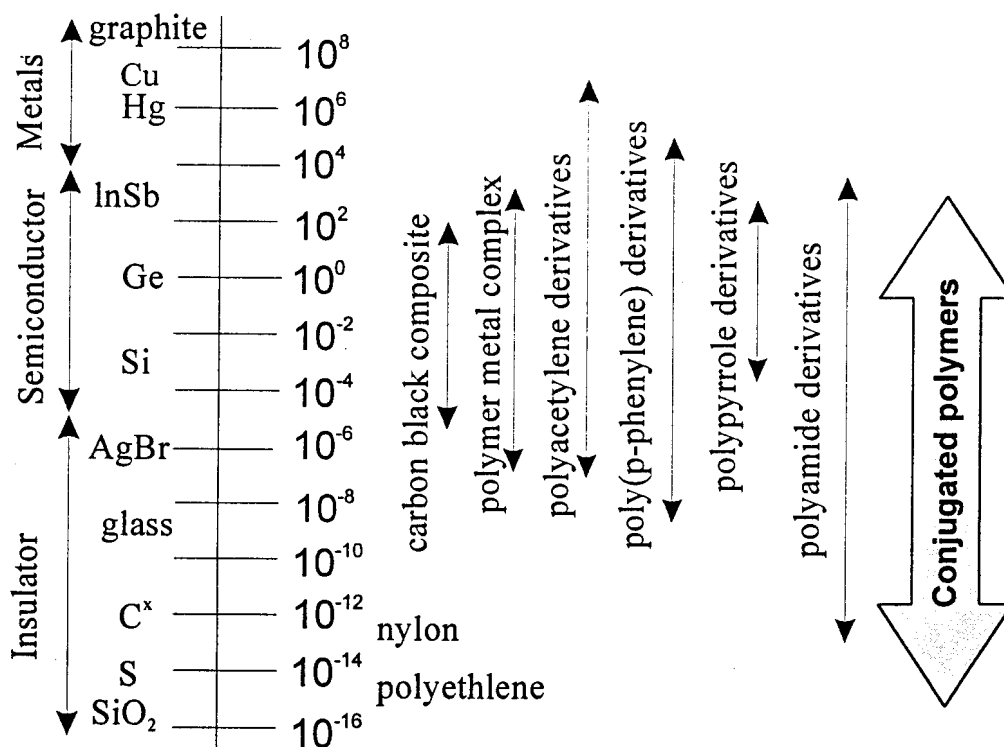


Fig (2.8): Conductivities (S/cm) of various elements, compounds and polymers²².

2.6 Improvements in polymer conductivity

The attainable conductivity of CPs increased steadily up until about 1992, through improvement in the synthesis and doping techniques as shown in figure 2.9. In the early 1980s the observed conductivity range for polyacetylene was $10^2 - 10^3$ S/cm, whereas since 1990 samples of polyacetylene with conductivities of approximately 10^5 S/cm are routinely produced²³. Highly conducting CPs (e.g. 10^5 S/cm for polyacetylene) are found to be unstable and therefore not suitable for device fabrication. As a result, highly conducting CPs are mainly used for charge transfer studies in the metallic region. Hence, not much research is centered at attaining extremely high conductivity

Since 1992, the conductivity of iodine doped polyacetylene has not improved beyond that of copper (slight improvements but not of much significance. This might have been achieved through varying conductivity determining variables such as stretching of the polymer and humidity).

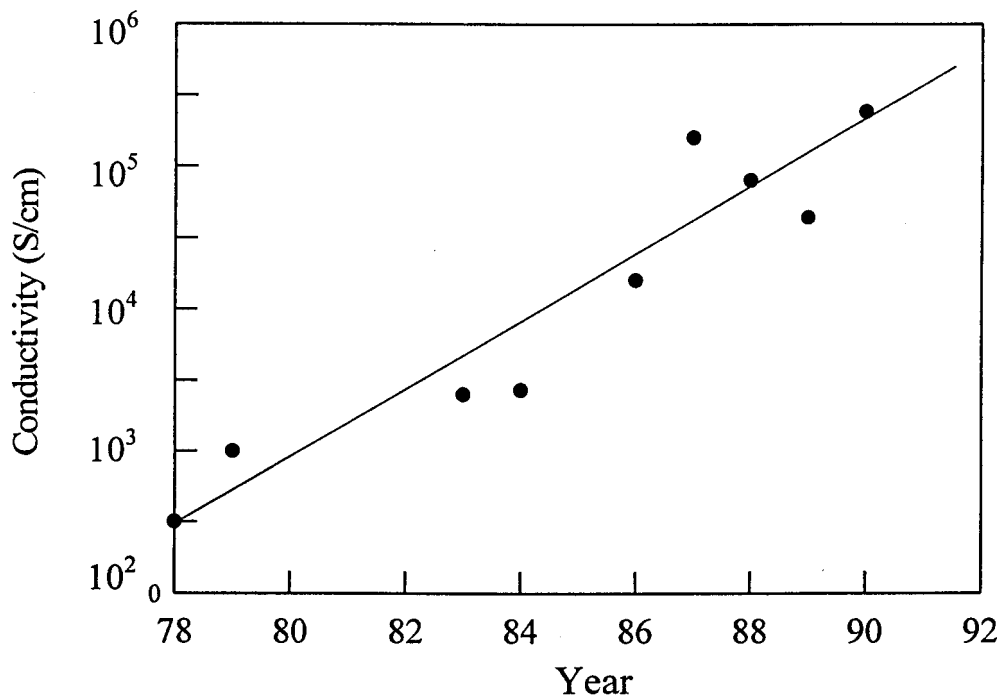


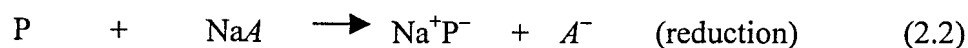
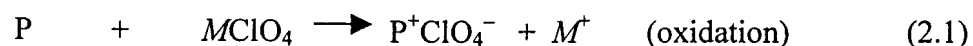
Fig (2.9): Advances in the conductivity of doped polyacetylene⁵.

An important contributing factor to the conductivity of CPs is improvements in the polymer morphology. A number of factors, such as molecular weight, plasticizer used, molecular weight distribution and crystallinity, have an influence on the morphology of the polymer and thus conductivity.

2.7 Doping and dopants

Pristine (undoped) CPs can be transformed from their insulating state to either a semiconducting or metallic state through the process of doping. Because of the semiconducting band structure of CPs electron removal/addition from the valence to the conduction band is possible leading to most of the properties that are of interest in CPs. The process of doping both in inorganic and organic materials can impart conductive properties to the material. However, as shall be illustrated, doping is in effect proper oxidation and reduction, in a chemical and electronic sense and not doping/dedoping in the inorganic semiconductor sense²¹.

The doping process leads to the presence of delocalized charges on CPs. These charges lead also to the relaxation of the geometry of the polymer to a more energetically favored conformation. Oxidation (anionic doping/*p-type*) generates a positively charged CP and an associated anion, while reduction (cationic/*n-type*) generates a negatively charged CP and an associated cation. These processes are illustrated below in equations 2.1 and 2.2, where *M* and *A* are any cation and anion, respectively and P represents a polymer²¹:



2.7.1 Dopants

Dopants are chemical oxidants or reductants incorporated into the CP by means of chemical, electrochemical, radiation and or at the time of synthesis²¹. Table 2.1 depicts some of the dopants used in chemical and electrochemical doping. The dopant is positioned on the chain so as to neutralize the charge formed from the oxidation or reduction doping reactions.

Table 2.1: Typical dopants for CPs²¹

<i>Dopant</i>	<i>Structure/formula</i>
<i>Anionic</i> (p-type)	Cl ⁻
Chloride	ClO ₄ ⁻
Perchlorate	BF ₄ ⁻
tetrachloroborate	CH ₃ -C ₆ H ₅ -SO ₃ ⁻
Tos, p-toluene sulfonate	[-CH ₂ CH(C ₆ H ₄ SO ₃) ⁻] _n ⁿ
<i>Cationic</i> (n-type)	
proton	H ₃ ⁺ O
sodium	Na ₊

The proportion of dopant ions incorporated into the polymer per monomer unit gives a measure of the doping level. Increased doping can lead to increased conduction, via the creation of more mobile charges, and the maximum doping levels achievable vary for different CPs and different dopants. Some representative doping maxima are listed in table 2.2.

Table 2.2: Typical maximum doping level

<i>Polymer</i>	<i>Maximum doping level</i>
Polyaniline	42% (Cl ⁻)
Polypyrrole	33% (ClO ₄ ⁻)
Poly(thiophene)	44% (Li ⁺)
Poly(p-phenylene)	30% (ClO ₄ ⁻)

2.7.2 Doping techniques

Among the most common doping techniques used are ion implantation, photochemical doping, heat treatment, solution doping and dry doping. In this study, we made use of electrochemical doping and chemical doping. We shall describe one of the two doping techniques used in the present work, namely electrochemical doping²¹.

The partial removal of electrons (oxidation) from the polymer π system is referred as p-doping, and n-doping refers to the addition of electrons (reduction) of the polymer π^* system. In electrochemical doping, if a positive potential is applied to a CP immobilized on an inert anode electrode, the dopant anion moves in from the solution into the CP towards delocalized charge sites on the CP, and anionic (*p-type*) doping occurs. Oxidation produces a polycationic chain, requiring the presence of anions from the oxidizing medium for charge compensation²¹ (figure 2.10). The counter ion is classified as dopant. Both *p* type and *n*-type dopants are possible for most CPs (see also equations 2.1 and 2.2).

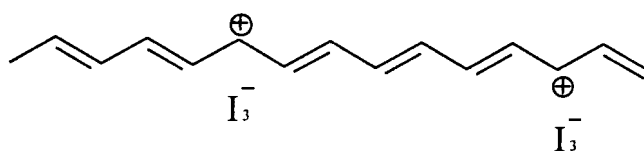


Fig (2.10): Negative ions are brought into the chain to neutralize a positive charge formed from the oxidant doping process. Iodine (I_2) will extract an electron under formation of an I_3^- ion in polyacetylene. See also figure 2.11.

The doping/dedoping reactions and the position of dopant anions (ClO_4^-) on the Pan chain are illustrated in figure 2.11.

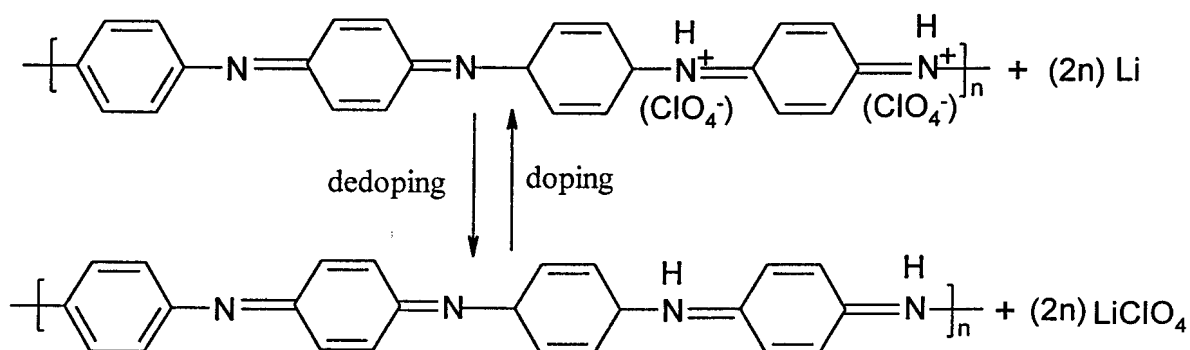


Fig (2.11): The doping and dedoping reactions of Pan⁸.

2. 8 Conducting polymer ionization

Conductivity in intrinsic CPs is enhanced partly through the process of doping. Because of the polymeric nature of these organic systems, the polymer is susceptible to structural distortions. The introduction of charge during the doping process leads to a structural distortion of the polymeric structure in the region of the charge, giving an energetically favorable conformation²¹. These structural distortions are intrinsic to the development of states called polarons, bipolarons and solitons. The effects of this structural relaxation can best be visualized by first considering ionization of an organic molecule according to the Franck-Condon treatment, as depicted in Figure 2.12.

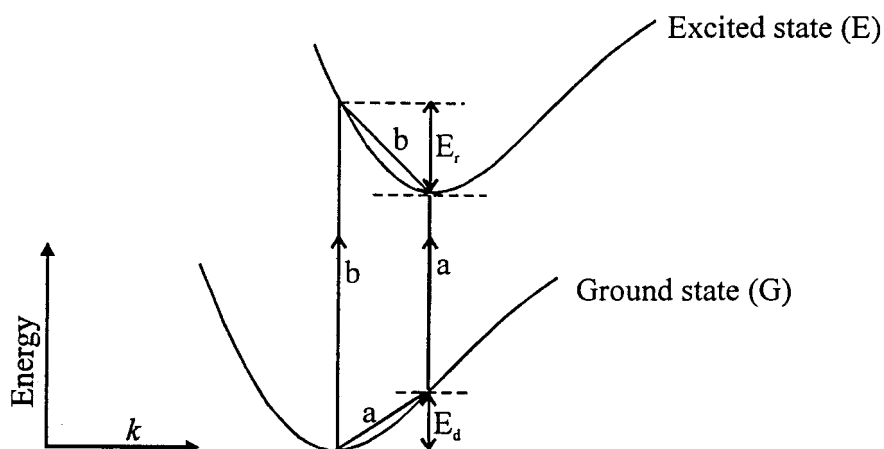


Fig (2.12): Ionization of an organic molecule according to the standard Franck-Condon treatment²¹.

Ionization can be thought to occur first through the excitation of the ground state (G) to the excited state (E). According to convention, the excited state, E , has a different geometry compared to that of the ground state G . Two possible routes (ionization processes) are:

- i. An initial distortion of the ground state geometry to that of the excited state, followed by the vertical excitation of the electron (*Path a*) or
- ii. A standard vertical Franck-Condon excitation (*Path b*) within the geometry of the ground state followed by relaxation to the equilibrium excited state geometry²¹.

If the excitation energy E_r is greater than the distortion energy, E_d , then path b is preferred for ionization.

2.9 The Fermi level

The Fermi level, E_F , in CPs is an equilibrium energy level corresponding to the chemical potential of the system and lies between the valence and conduction bands (π and π^* orbital bands respectively). Unlike in inorganic materials, an increase in

conduction as a result of doping corresponds to the upward and downward shift of the HOMO and LUMO bands, respectively, decreasing the bandgap in the process²¹, figure 2.13.

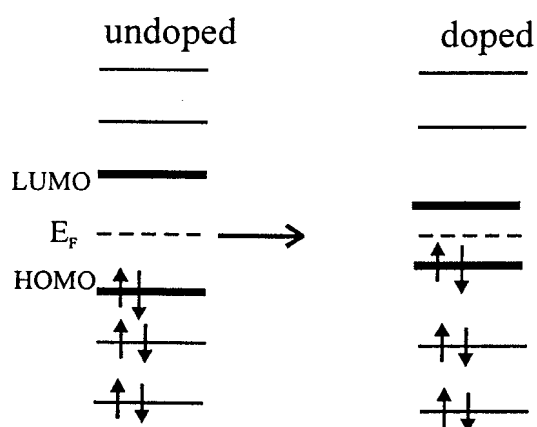


Fig (2.13): The effect of the doping process on the position of the HOMO, LUMO and the Fermi level (E_F)²¹.

2. 10 Band structure treatment

The electronic conductivity of CPs is explained using the semiconductor bandgap model to describe the energy levels available to a material's charge carriers. An understanding of the band structure of CPs is important for one to be able to appreciate why CPs are described by the same treatment as inorganic semiconductors.

The ground state of a CP is that of an insulator, with a forbidden energy gap between filled and empty energy levels¹⁴. The energy gap arises from the pattern of single (long) and double (short) bonds with an additional contribution due to electron – electron Coulomb repulsion¹⁴. An overlap of the HOMO and LUMO bands results in metallic conduction^{21, 2, 23}. The bandgap in doped-CP systems varies from 1eV to 4eV², coupled with other measured parameters. In general, doped conjugate polymers behave like inorganic semiconductors. Unlike inorganic semiconductors, the band structure of CPs has flexibility and is susceptible to structural distortions²¹.

The doping and dedoping effects in CPs can be analyzed fully in terms of bandgaps, such as in inorganic semiconductors. Bredas *et al.*^{1, 2} have extensively studied the spectral evolution of polypyrrole as a function of doping level. An elementary experiment based on band theory involves initially holding the polymer in its fully reduced state at a potential of 0.0 V and thus its electronic absorption from 350 nm to 2500 nm. Subsequently, the potential is stepped anodically to *p*-dope the polymer with a spectrum recorded at each potential step.

The results obtained indicate that there is one strong absorbency due to π - π^* transitions of the neutral polymer. These results are satisfactorily explained with the help of the energy band diagram illustrated in figure 2.14.

From figure 2.14, there are four optical transitions possible, in decreasing order of energy: 1) From the valence band (VB) to the conduction band (π - π^* transition); 2) from the valence band to the upper polaron level; 3) from the lower polaron level to the upper polaron level; 4) and from the valence band to the lower polaron level. In the case of bipolarons the transition between polaron levels is eliminated.

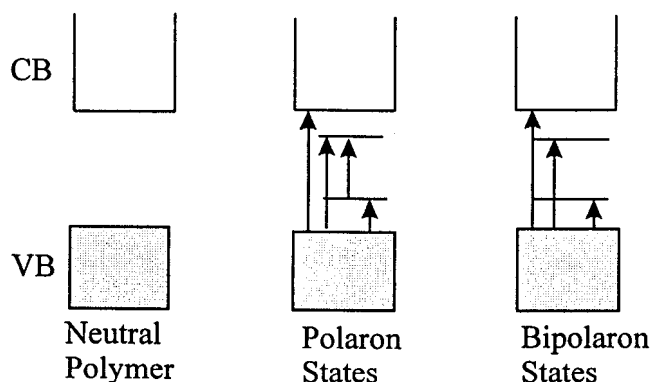


Fig (2.14): Band diagram for the optoelectrochemical spectra of a CP²¹.

2.11 Structural distortions: Polarons, bipolarons and solitons

The introduction of dopant ions into the polymer, as mentioned in the previous sections, results in the creation of two localized midgap states within the bandgap. Oxidation and/or reduction processes result in the creation of charged carriers called solitons, polarons and/or bipolarons²¹. The effect of doping and doping level on the creation of such defects and their position in the bandgap are detailed below.

2.11.1 The polaron band theory

When an electron is added to a perfect chain, it causes the chain to deform, creating a characteristic pattern of bond deformation. Along with the chain deformation, there is a change in the energy level structure. An energy level is pulled out of the valence band into the gap between the valence and conduction band edges and another level is pulled out of the conduction band to form two polaron band levels or states (fig. 2.14)⁹, the lower polaron level is occupied by two electrons of opposite spins as illustrated in figure 2.15a.

2.11.2 Polaron formation

As explained above localized distortion gives rise to localized electronic states in the bandgap region. Removal of a single electron from this localized state through doping results in the formation of a positive polaron, while the addition of an electron results in a negative polaron (figure 2.15 (b) and (c) respectively). The polaron as shown is a radical cation, which is associated with a structural distortion in the CP. Since we have a single charge, the lower bipolaron level is half-occupied, as shown and the species would possess spin. The half-occupied, electronic level (polaron) remains localized in the gap²¹.

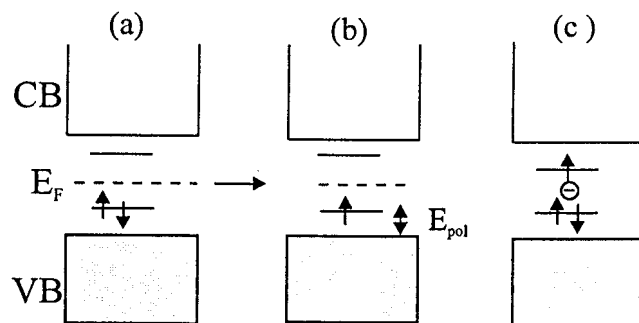


Fig (2.15): Formation of a polaron; (a) localized electronic states, (b) positive polaron formed from oxidative doping and (c) negative polaron formed from reductive doping²¹.

Another approach towards the formation of a polaron will be to consider the removal of an electron from the CP structure resulting in a localized distortion in the structure, which then serves to stabilize the charge associated with the electron removal. The distortions of the local structure by a charge in an extended lattice arises from electron-phonon coupling. The polaron is said to possess binding energy equal to $E_{pol} - E_{dis}$, where E_{dis} is the distortion energy and E_{pol} is the difference in energy between the polaron level and the valence band (VB)²¹.

2.11.3 Bipolaron formation

The removal of a second electron from the polaron results in the formation of a bipolaron, figure 2.16. This bipolaron is stable despite Coulomb repulsion of the two similar charges. The stability of the bipolaron is thought to arise from coupling of the two charges to the lattice via lattice vibrations and neutralization of the repulsion between the charges by the dopant ions. In figure 2.16, E_{bip} is the bipolaron binding energy.

Oxidative and reductive doping gives rise to positively and negatively charged bipolarons respectively, figure 2.16.

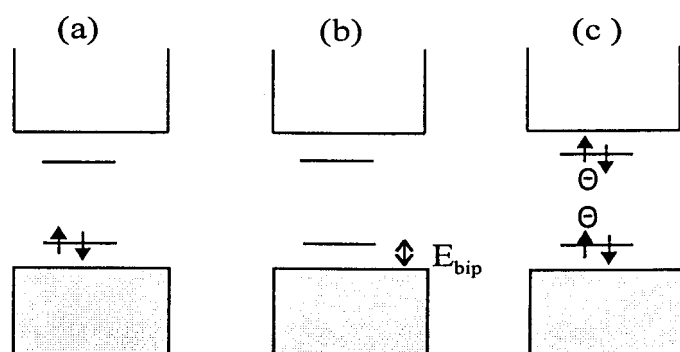


Fig (2.16): Formation of bipolaron: (a) localized electronic states, (b) positive bipolaron formed from oxidative doping of a polaron and (c) negative bipolaron formed from reductive doping of a negative polaron²¹.

Bipolarons are either empty (p-doped) or full (n-doped) and thus they are spinless. In the formation of the polaron/bipolaron, the conduction band remains full and the valence band empty, therefore the high conductivity comes from diffusive motion of these bipolarons. Doped CPs exhibit strong anisotropy of conductivity along the polymer chains through the migration of charged defects coupled to a local deformation of the π -conjugated structure (polaron/bipolaron)⁹.

2.11.4 Soliton

A soliton is an excitation that occurs only in degenerate polymers (polymers with which the exchange of single and double bonds does not result in a higher energy state). To define a soliton, let's consider trans-polyacetylene (t-PA) schematically shown in figure 2.17. With double bonds sloping to the right, as shown, take this as "A" and the one with double bonds sloping to the left as "B". A type "A" region can occur next to a type "B" region on the same t-PA chain⁴. There exists a region between them upon which a transition takes place, (see also figure 2.10).



Fig (2.17): Right and left sloping double bonds for t-PA²⁴.

The domain wall between different directions of the double bond, i.e. between “A” and “B”, is called the soliton. A bound electron characterizes it. This bound electron, which is neither bonding nor anti-bonding, occupies a level at the center of the energy gap. Therefore a new energy level is created with a reduced energy gap. Electrons can be promoted from the valence band to the conduction band through the formation of solitons. When there is an odd number of carbon atoms in the CP chain, there remains an unpaired π -electron, and a radical, neutral soliton is said to result²¹. The schematic band structure for neutral, positive and negative solitons respectively is shown in figure 2.18.

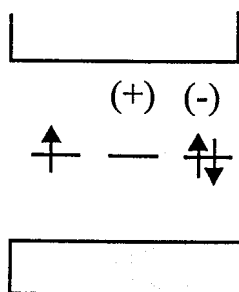


Fig (2.18): Neutrally, positively and negatively charged solitons²¹.

The soliton level can accommodate zero, one and/or two electrons and thus it may also be positively or negatively charged, giving the unusual property of separating spin and charge, with neutral solitons possessing spin; but no charge. Both positively and negatively charged solitons possess charge but no spin. For doped CPs, charge is located in the mid-gap states, since these provide the HOMO for the charge removal and the LUMO for charge injection²¹. However, because various kinds of defects in polymers, such as crosslinks between chains and bends, and kinks, are common, conduction should

be to a larger extent a combination of the three modes described above in most of the cases.

2.11.5 Polarons, bipolarons and solitons in a polymer chain

Polarons, bipolarons and solitons are confined to, and delocalized over, about four to six monomer units. A counter-ion (dopant ion) is located in the vicinity of the entity for charge neutrality²¹, as indicated previously for the case of Pan (figure 2.10). The appearance of these defects in the polymer chain is shown in figure 2.19.

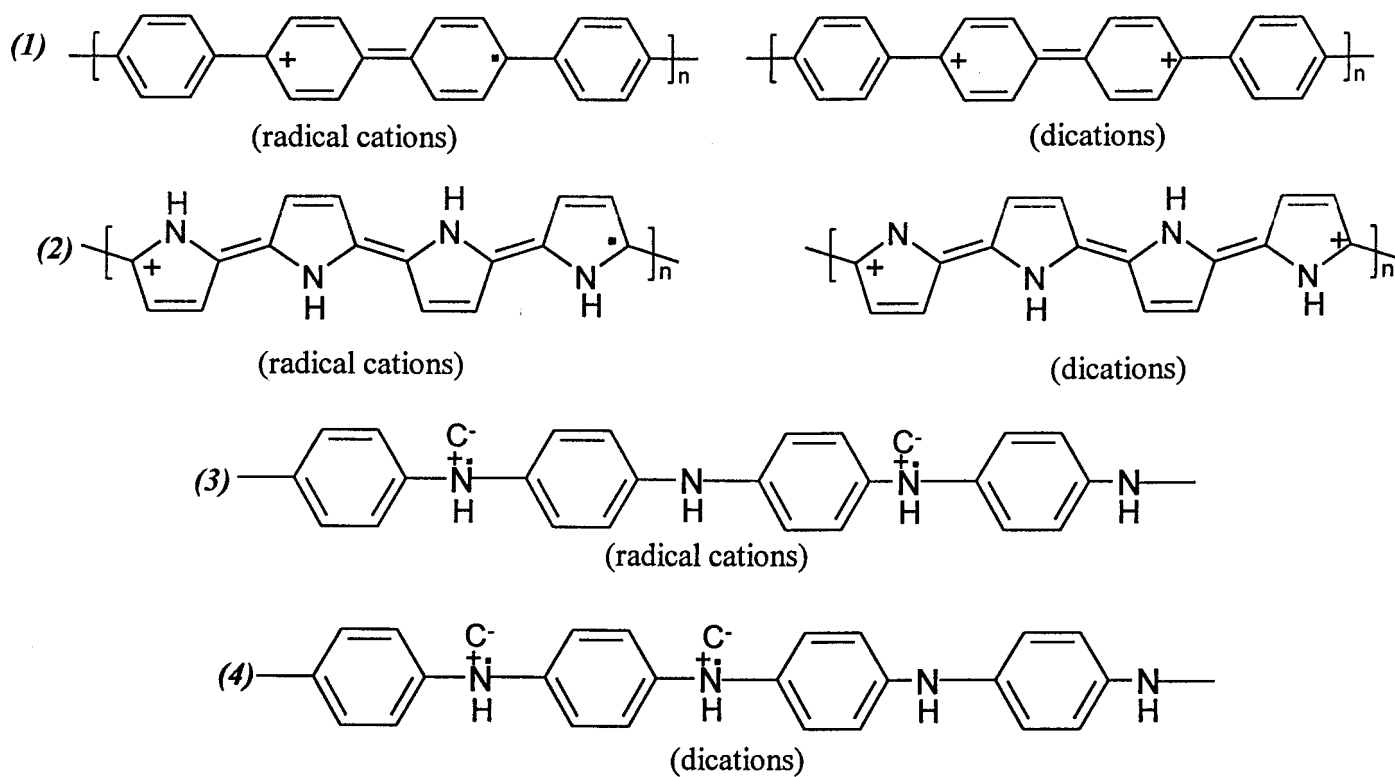


Fig (2.19): Polarons (radical cations) and bipolarons (dications) for (1) PPV²¹, (2) polypyrrole²¹ and Pan⁸ (3) and (4) respectively.

2.12 Band structure evolution

Figure 2.20 depicts the evolution of band structures, (polypyrrole taken as an example), based on semi-empirical theoretical and experimental studies on CPs, first presented by Bredas *et al*^{1,2}. Removal of an electron from the polymer chain produces a polaron, with two-polaron levels at about 0.5eV from the conduction and valence band edges, according to the approximate calculations of J. Bredas *et al*²¹.

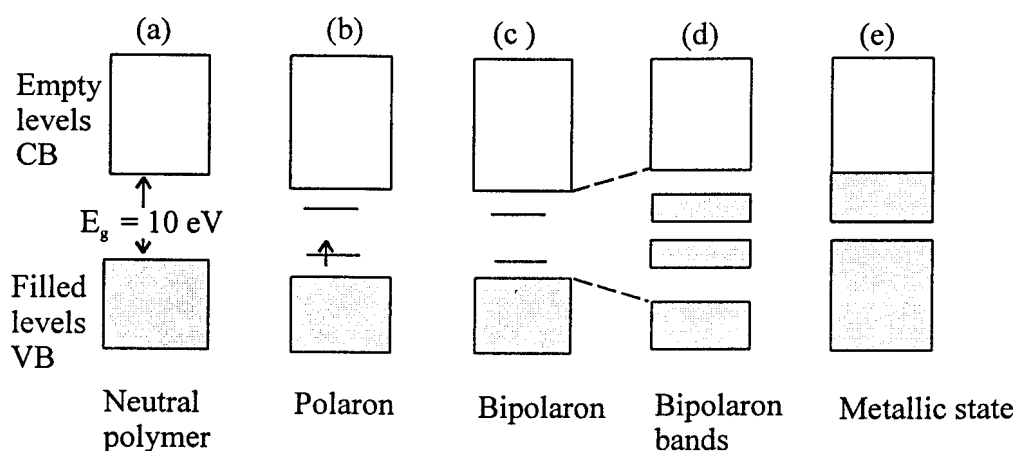


Fig (2.20): Hypothetical evolution of band structure to a metallic state for CPs²¹.

The polaron has a band structure like that depicted in figure 2.20, with the single positive charge delocalized over about 4 to 6 monomer units. Removal of a second electron produces a bipolaron²¹. On increased doping (a maximum of about 35 % for polypyrrole), the individual bipolaron states of figure 2.20 (c) coalesce into bipolaron bands (figure 2.20 (d)). Bipolaron bands arise from electronic states taken from the valence and conduction band edges, and the gap between these bands consequently increases.

Assuming a hypothetical doping level of 100 % (one dopant ion per monomer unit), the two bipolaron bands would gradually broaden enough to coalesce into the valence and conduction bands (figure 2.20(e)), producing metal-like conduction²¹. At these high dopant concentrations, the bipolarons, which are spinless, can become mobile under the application of an electrical field, thus giving rise to high conductivity.

The width of the polaronic levels are affected by the influence of chains of different length, disorder, interchain coupling, electron-electron interactions, and interactions between chains and dopants¹.

In summary, this chapter aims at giving a comprehensive introduction to the study of conducting polymers. A description of the molecular structure concomitant with conductivity in this special type of polymers is detailed. Following is the description of charge carriers and the process of conduction enhancement. CPs have the same band gap structure as other inorganic semiconductors and their conductivity can also be improved through the process of doping.

References

1. J. L. Bredas, J. C. Scott, Phys. Rev. **B 30**, 1023 (1984).
2. J. L. Bredas, D. Beljonne, Z. Shuai, Conjugated Oligomers and Dendrimers, From PA to DNA, (Ed. J. L. Bredas), De Boek Universite: Paris (1998).
3. U. Sum, H. Buttner, Phys. Rev. **B 40**, 6166 (1998).
4. C. Trivedi, Handbook of Organic Conductive Molecules and Polymers **2** (Ed. H. S Nalwa), John Wiley and sons: New York, 506 (1997).
5. J. Tsukamoto, Adv. in Phys. **41**, 509 (1992).
6. T. F. Otero, Handbook of Organic Conductive Molecules and Polymers **4** (Ed. H. S Nalwa), John Wiley and sons: New York (1997).
7. K. Gurunathan, Materials Chemistry and Physics **61**, 173 (1999).
8. A. J. Epstein, A. G. MacDiarmid, Science and Application of conducting polymers, (Ed. W. R. Salaneck), Bristol: England (1991).
9. E. Conwell, Handbook of Organic Conductive Molecules and Polymers **4** (Ed. H. S Nalwa), John Wiley and sons: New York (1997).
10. Source: Internet: WWW.lumex.com/tech_notes/polymer.htm
11. M. Rusu, G. Rusu, Appl. Surf. Sc. **126**, 245 (1998).
12. A. G. MacDiarmid, Synth. Met. **84**, 27 (1997).
13. P. Yam, Trends in Material Sc. (Scientific American), **75**, July (1995).
14. A. J. Epstein, MRS Bulletin, **22**, 16 (1997).
15. E. Kim, K. Lee, S. B. Rhee, J. Electrochem. Soc. **144**, 227 (1997).
16. C. Arbizzan, B. Scrosati, Handbook of Organic Conductive Molecules and Polymers **4**, (Ed. H. S Nalwa), John Wiley and sons: New York (1997).
17. Y. Yang, MRS Bulletin **22**, 31 (1997).
18. B. Wessling: source: www.zipperling.de/Research/abstract/corros
19. R. Menon, Handbook of Organic Conductive Molecules and Polymers **4**, (Ed. H. S Nalwa), John Wiley and sons: New York (1997).
20. Chemistry a study of matter, (Ed. A. B. Garret), Xerox corporation: Toronto (1972).
21. Conducting polymers, Fundamentals and Application, (Ed. P. Chandrasekhar), Kluwer academic publishers: Boston (1999).

22. S. R. Sethi, M. T. Goosey, Elec. Prop. of polymers, 1, Ed. C. C. Ku (1993).
23. D. O. Cowain, F. M. Wlygul, C & EN, 28, July, (1986).

1*. M.E. Jozefowcz, R. Laversanne, H. H. Javadi, J. A Epstein, A. G. MacDiarmid, Phys. Rev. **B 39**, 12958 (1989).

2*. U. Sum, H. Buttner, Phys. Rev. **B 40**, 6166 (1988).

3*. R. P. McCall, J. M. Ginder, A. G. MacDiarmid, Phys. Rev. **B 41**, 5202 (1990).

3*. J. M. Ginder, J. A Epstein, Phys. Rev. **B 41**, 10674 (1990).

4*. J. L. Bredas, J. C. Scott, Phys. Rev. **B 30**, 1023 (1984).

Chapter 3

The structure and properties of different forms of Pan

In the group of materials known as CPs, polyaniline (Pan) an oxidative polymeric product of an aniline under acidic conditions is one of the more studied materials due to its:

- (1) Easy synthesis¹
- (2) Environmental stability¹
- (3) Simple non-redox doping by protonic acids¹
- (4) Diversified applications^{1,2}
- (5) Can assume diverse incarnations, including thin films and patterned surfaces²

Pan is a phenylene-based polymer with a chemically flexible –NH– group in a polymer chain flanked on either side by a phenylene ring¹. The –NH– group is important for the physico-chemical properties of Pan such as the protonation and deprotonation (non-redox doping). This non-redox doping by protonic acids is an important aspect where a number of electrons in a polymer chain remain unchanged during the doping process. The protonated form is electrically conducting, and the magnitude of increase in its conductivity is a function of the level of protonation as well as the functionalities present in the dopant¹.

Pan and its related CPs such as poly (p-phenylene oxide) PPO and poly (p-phenylene sulfide) PPS have been shown to contain large equilibrium phenyl ring torsional displacements (upwards of $\pm 30^\circ$ or more) out of the plane defined by the ring bridging atoms (amine/imine nitrogens in the case of Pan and sulfur for PPS)². The chemical and structural flexibility surrounding the amine/imine nitrogen linkages in Pan creates enormous diversity: the geometry, electronic structure, and dynamics of the defect states are quite different from those of the carbon-backbone-conjugated polymers. There is an

overall reduction in the effective intrachain conjugation length and a marked decrease in the tendency to form crystalline phases. This also implies that there are implications to the electronic transport properties of the polymer². Despite the experimental evidence for the long-lived massively charged defects in Pan, as well as the demonstration of the importance of ring flipping as a relaxation mechanism, the role of ring conformational changes in the self-trapping of charged defect states has received little attention². Ring flipping shall be illustrated together with the conventional representation of the molecular structure of polymers in the following sections.

In order to form a reasonable understanding of CPs, knowledge of the structure and terminology used is necessary.

3.1 The different forms of Pan

Pan can be transformed through four different oxidation states, each oxidation state having different electronic and optical properties. The different forms of Pan are determined⁴ by the fraction of imine ($-NH=$) nitrogen atoms per 4-ring repeat unit, which is labeled $1-y$. Where $1-y$ is equal to 0.5, 0 and 1 for half-oxidized (emeraldine), fully reduced (leucoemeraldine) and fully oxidized (pernigraniline) forms, respectively. The chemical formula which most broadly describes this polymer is presented in figure 3.1.

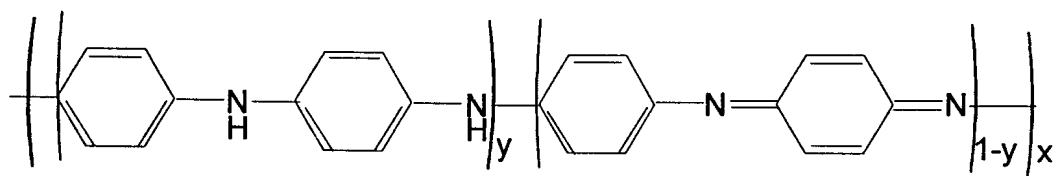


Fig (3.1): The base form of Pan: leucoemeraldine ($y = 1$), emeraldine ($y = 0.5$), and pernigraniline ($y = 0$)⁵.

The emeraldine base (EB) insulating form of Pan is the most important form, because it can be doped to high conductivity and it is easily processible in this state (that is through dissolving it in appropriate solvents). The comparison of Pan to other CPs is based on the

EB form of Pan. The EB form differs substantially from other CPs in several important aspects:

1. The C_6 benzoid rings of Pan can rotate or flip, significantly altering the nature of electron – phonon interactions⁶.
2. Emeraldine can be converted from an insulating to a metallic state if protons are added to the $-N=$ sites while the number of electrons on the chain is held constant⁶.
3. Pan comprises an alternating ring-heteroatom backbone structure. Both carbon rings and nitrogen atoms are within the conjugation path, forming a generalized “ $A - B$ ” polymer^{4,6}.
4. It does not display charge conjugation symmetry in contrast with the most studied polymers polyacetylene and polythiophene⁶.
5. The polymerization mechanism affects the properties in as much as it influences the microstructure, the molecular weight and the molecular weight distribution⁴.

A summary of the properties of the different forms of Pan is shown in table 3.1.

Table 3.1: Forms of Pan and their electrical properties

<i>Forms</i>	<i>Oxidation state</i>	<i>Electrical properties</i>
Emeraldine base (EB)	Half-oxidized	Can be doped to high conductivity
Emeraldine salt (ES)	Half-reduced	Conducting
Leucoemeraldine base	Fully reduced	Insulating
Pernigraniline base	Fully oxidized	Insulating

Pan has excellent electrochemical reversibility and stability in aqueous media. The color of a Pan film in aqueous solutions can change very quickly with applied potential. In a solution containing $ZnCl_2$ and NH_4Cl , at $pH > 4$ in a phosphate buffer, the color of Pan film changes from reddish purple to blue—*fully reduced*, green—*half oxidized*, and transparent yellow—*fully oxidized states* when the potential is swept from 0.8 to -0.10 V⁷. A detailed description of each of these forms is presented in the coming sections.

3.1.1 Emeraldine base (EB)

This is a half-oxidized insulating Pan with a large extrinsic gap ($E_g \sim 3.6$ eV) and $1-y = 0.5^4$ (fig. 3.2). EB can be converted from an insulating to a metallic state if protons are added to the $-NH=$ sites while the number of electrons in the chain are held constant⁶. Because of this property, EB is the most important form of Pan.

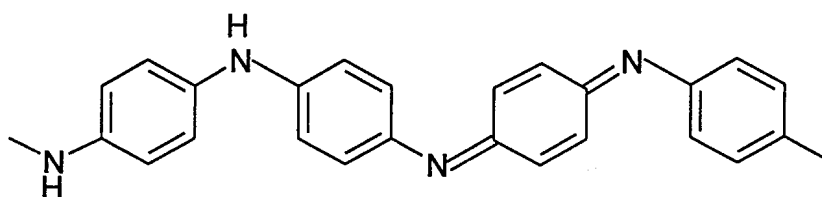


Fig (3.2): Emeraldine base structure.

The degree of crystallinity is typically low and, even in the best samples, never exceeds 50 %. In the approximate structure of Jozefowicz *et al.*⁸, the deviation from planarity by the phenyl rings is sequentially alternated between $\pm 30^\circ$ as one moves along the backbone as illustrated in figure 3.3.

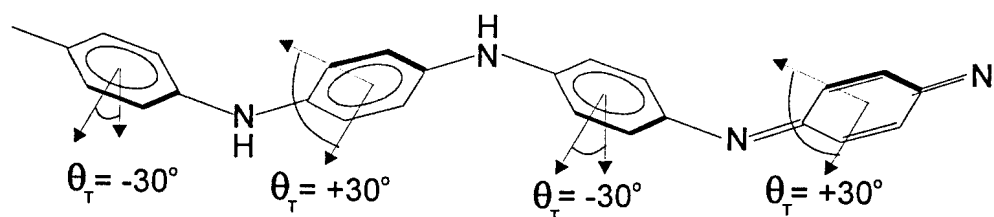


Fig (3.3): Schematic diagram of a four-monomer repeat in Pan EB showing the deviation from planarity of the four rings, three benzoid and one quinoid for crystalline EB⁸.

3.1.2 Leucoemeraldine base (LEB)

In the LEB form illustrated in figure 3.4, Pan exists in the fully reduced state, $1-y = 0$. LEB is an insulator whose large extrinsic energy gap ($E_g \sim 3.6 \text{ eV}$)⁹ originates predominantly from the difference in energy between the bonding and anti-bonding molecular orbitals of benzene involved in the overlap of molecular orbitals of neighbouring phenyl rings and nitrogen atoms.

The presence of amine (-NH-) groups allows chemical flexibility so that other electronic states of the polymer can be obtained by removal of protons (or hydrogen atoms), as well as electrons, from the polymer⁴.

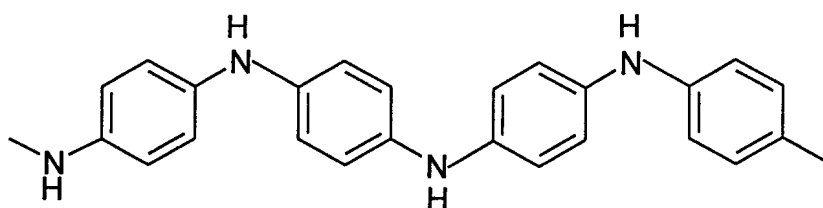


Fig (3.4): Leucoemeraldine base structure⁴.

The ground state configuration of LEB consists of adjacent phenyl rings twisted out of the nitrogen-nitrogen plane by equal but opposite angles, $\theta \sim \pm 30^\circ$ figure 3.5^{9,10}. Changes in the number of electrons along the polymer backbone results in new ring angles which

are different from the ground-state configuration. p-Doping of LEB results in the formation of a hole polaron, (P^+) described as a ring-centered distortion in which the center phenyl ring twists out of its ground-state configuration toward the plane formed by the nitrogens. This distortion causes neighboring rings to distort toward planarity and away from the ground-state angle; figure 3.5¹⁰.

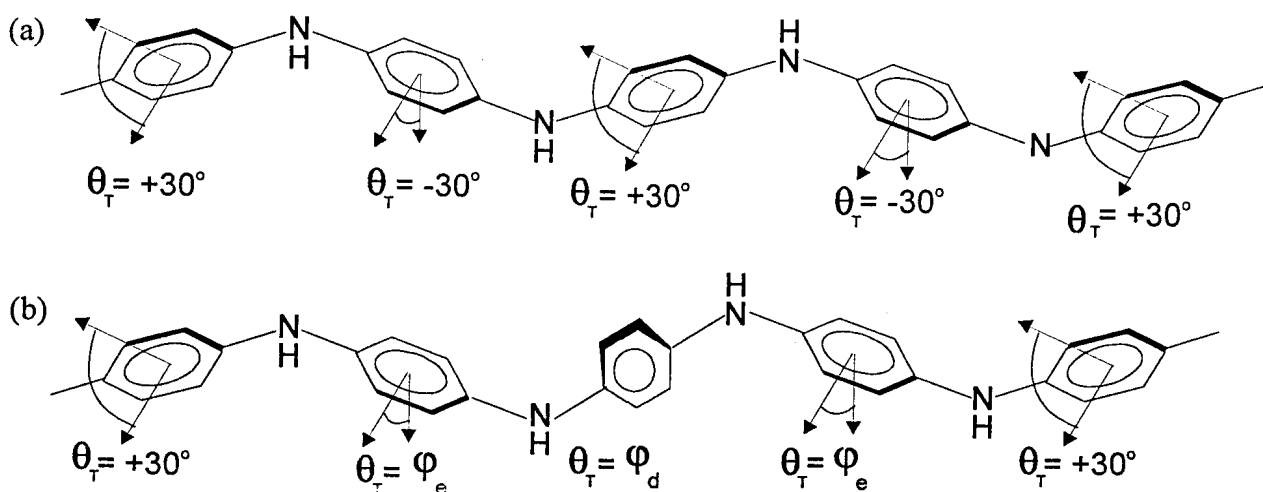


Fig (3.5): (a) A segment of a LEB chain showing the phenyl rings rotated by $\pm 30^\circ$ out of the plane formed by the nitrogens. (b) Representation of a ring-rotational hole polaron in LEB where the center phenyl ring and the phenyl rings rotate toward the nitrogen plane to new angles φ_d and φ_e ¹⁰

A negative polaron (P^-) causes almost no ring-rotational effects, although bond-length effects produce very small asymmetrical splittings from the conduction and valence bands less than a few tenths of an eV¹⁰.

3.1.3 Pernigraniline base (PNB)

This fully oxidized ($1-y = 1$) and insulating form of Pan, shown in figure 3.6, has an energy gap ($E_g \sim 2.3$ eV) that is intrinsic due to electron-phonon interactions⁴. The electronic structure of PNB is characterized in terms of a Peierls ground state¹⁰ that supports soliton and polaron defects. The half-filled π -band is split by an energy gap caused by an effective bond-length alternation, resulting in the constituent phenyl rings of

the Pan backbone taking on an alternating quinoid-benzenoid character analogous to the double-bond-single-bond alternation in dimerized *trans*-polyacetylene¹⁰. The resulting degenerate ground state of PNB supports bond-alternation defects, particularly solitons and polarons, which accommodate doping-induced and photo-induced charge in the polymer¹⁰.

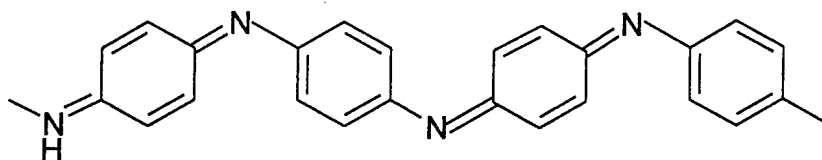


Fig (3.6): Pernigraniline base structure⁴.

3.1.4 Emeraldine salt (ES)

ES is the conducting form of Pan formed by the protonation of EB by exposure to protonic acids (a process which is a variation of either the number of protons, electrons or both (*on the unprotonated $-N=$ sites*) or on n- and /or p- doping of LEB^{4,5}). Figure 3.7 shows the two processes leading to one form, ES. Doping causes the orders of the undoped insulating forms to change, resulting in a reorganized electronic structure described as a metallic polaron energy band¹¹.

The conductivity of pristine Pan increases by several orders of magnitude upon doping and depends on a number of factors including, dopant used and processing in different solvents¹¹. Upon protonation of the formerly unprotonated $-N=$ sites of EB, the conductivity increases by a factor of 10^{10} , reaching about 1S/cm, despite the unchanged electron concentration⁶.

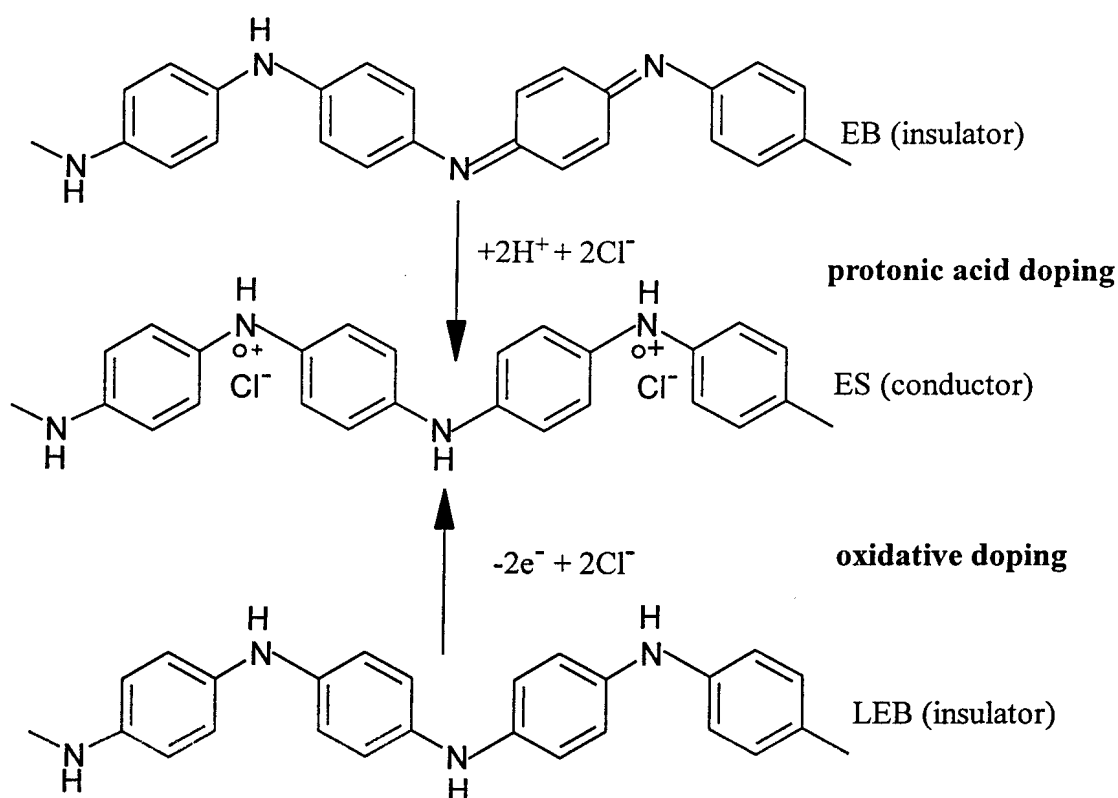


Fig (3.7): Illustration of the oxidative (*p*-doping) of LEB and protonic acid doping of EB, leading to the same final product, ES^{11} .

3.2 Polyaniline derivatives

The derivatives of Pan are obtained from doping the EB form of Pan with organic or inorganic acids, with the subsequent substitution of one of the benzene hydrogens by an anion from the acid. Pan derivatizing improves the material's processibility and compatibility¹⁰. Examples are: the sulphuric acid substituted derivative, where a hydrogen on the C_6 ring is replaced with a $\text{SO}_3^- \text{H}^+$ unit (figure 3.8), poly (orthotoluidine) POT-EB where a single hydrogen at the C_6 ring is replaced with a single CH_3 unit (figure 3.9)¹⁰, and the hydrochloric acid salt of POT-ES, (figure 3.9(b)). The covalent bonding of protonic acids to the Pan backbone gives important properties that are not available in the emeraldine hydrochloride (HCl doped Pan). $\text{SO}_3^- \text{H}^+$ substituted Pan (figure 3.8a and b) is

soluble in water and aqueous base media. Pan POT-EB has been useful in the study of the effects of ring derivatization and interchain electronic properties of the polymer^{6,12}.

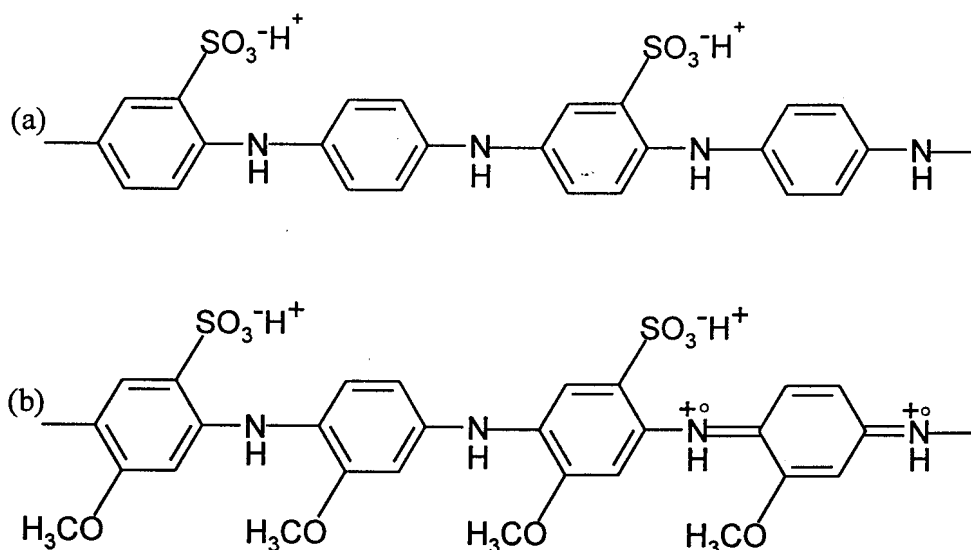


Fig (3.8): Schematic illustration of derivatives of Pan (a) 50% sulfonated and (b) 100% sulfonated Pan (self-doped forms)¹².

The interest in Pan stems from the fact that many different ring- and nitrogen- substituted derivatives can be readily synthesized and that each derivative can exist in several different oxidation states which can, in principle, be “doped” by a variety of different dopants either by non-redox processes or by partial chemical or electrochemical oxidation.

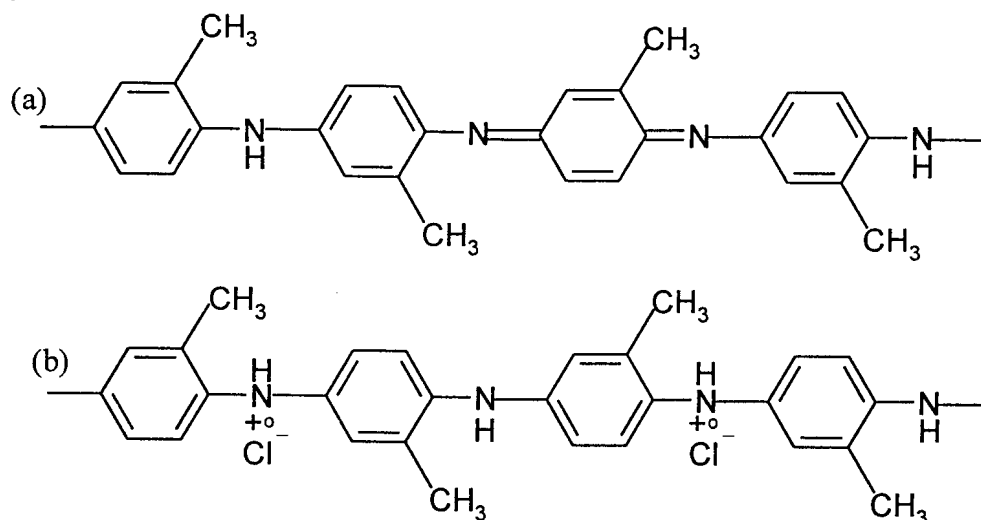


Fig (3.9): The structure of (a) POT-EB and (b) HCl salt of POT- ES derivatives of Pan¹².

3.3 Switching properties

The potential applications of Pan are related to the ability of this polymer to change its oxidation state, irrespective of the effect which induces this change: standard chemical or electrochemical oxidation and reduction, variation of the pH of the medium and effect of various types of energy (solar and radiation)². Variation of the oxidation state results in changes of the whole spectrum of chemical, physiochemical and physical properties of the polymer: oxidation potential, light absorption, dielectric constant, refractive index, acid dissociation constant (pK_a), conductivity, crystallinity, dimensionality and a number of properties not stated here².

The chemical, conductive and electrochromic properties of Pan, can be controlled by application of a potential and /or an acid or base. Pan switches vice versa from the fully undoped form, LEB, that is less conductive to fully oxidized PNB that is insulating upon reaction with acids or bases that protonate and deprotonate the base sites of the polymer¹³.

3.4 The polaron lattice of polyemeraldine

The geometric structural representation summarizing the formation of a polaron lattice in Pan is represented in figure 3.11. A model based on a two-step transition from isolated, doubly charged, spinless bipolarons to a polaronic metal [figures 3.11 (b) - (d)] was suggested by Stasftrom *et al*¹². The first step relates to the instability of a bipolaron on a polyemeraldine chain [figure 3.11 (b)], with respect to the formation of two polarons [figure (3.11(c)], and the second step is their separation to yield a polaron lattice¹¹.

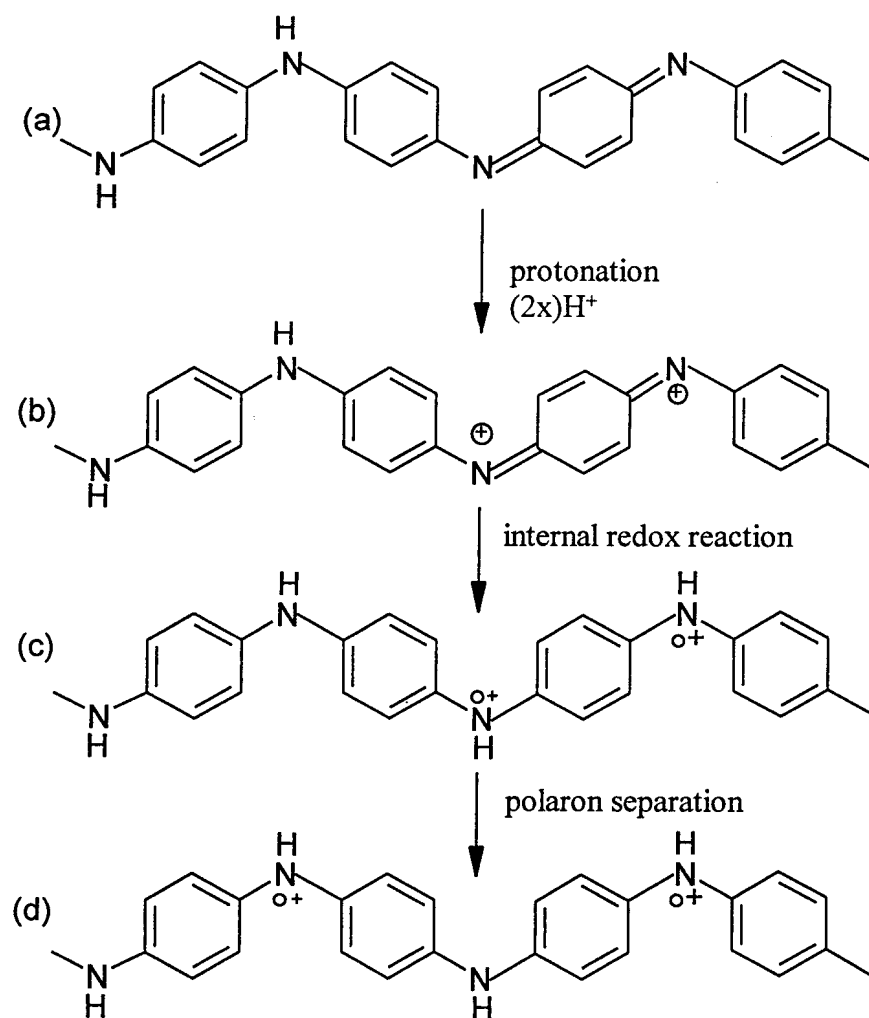


Fig (3.11): The geometric structure of Pan (a) before protonation and (b)-(d) after 50% protonation: (b) formation of bipolarons and (c) polarons; (d) the polarons separate, resulting in a polaron lattice¹¹.

3.5 The mass of charge carriers in polyaniline

The mass of polarons is very large $M_{\text{polaron}} > 60m_e$, where m_e is the mass of an electron¹³. Experimental evidence has shown that M_{polaron} increases with an increase in the moment of inertia of the rings through addition of substituents. A further increase in the defect mass may result from interchain effects (due to increased interchain distances), causing changes in the ground state and excited state ring angles, as well as an increase in the average ring angle resulting from an increased intrachain steric effect of the methyl groups in poly (*o*-toluidine)¹⁴. Table 3.2 lists the defect (polaron) masses for LEB, EB, PNB, and half-oxidized poly (*o*-toluidine)⁵.

Polarons, bipolarons and/or solitons are delocalized within a polymer chain and can travel along a chain as an entity, the atoms in their path changing their positions so that the deformation travels with the electron or hole. The fact that the atoms must move as these particles drift along a chain, results in an increase in the effective mass of the particles (table 3.2)¹⁵.

Table 3.2: Masses of long-lived defect states for various forms of Pan⁴.

<i>Material</i>	<i>Defect mass</i>
Leucoemeraldine base (LEB)	~ 60 m_e
Emeraldine base (EB)	~ 60 m_e
Pernigraniline base (PNB)	~ 300 m_e
Half-oxidized poly (<i>o</i> -toluidine) POT	~ 200 m_e

References

1. D. C. Trivedi, HandBook of Organic Conductive Molecules and Polymers 2 (Ed. H. S Nalwa), John Wiley and sons: New York (1997).
2. N. Gospodinov, L. Terlemezyan, Prog. Poly. Sci. **23**, 1443 (1998).
3. P. Yam, Trends in Material science, Scientific American, 75, July (1995).
4. J. Epstein, R. P. McCall, J. M. Ginder and A. G. MacDiarmid; Spectroscopy of advanced Materials, (Ed. R. J. H. Clark), Chichester: Wiley (1991).
5. A. J. Epstein, MRS Bulletin **22**, 16 (1997).
6. M. E. Jozefowicz, A. J. Epstein, A. G. MacDiarmid, Phys. Rev. **B 39**, 12958 (1989).
7. M. Shaolin, L. Jincui, www.chemistrymag.org/1999/011001pe.htm
8. <http://romano.physics.wisc.edu/winoku/>
9. J. Fan, D. Zhu, Solid state communications **110**, 5762 (1999).
10. R. P. McCall, J. M. Ginder, J. M. Lang, A. G. MacDiamird; Phys. Rev. **B 41**, 5202, (1990).
11. S.Satafstrom, J.L.Bredas, Phys. Rev. Lett. **59**, 1464 (1987).
12. A. J. Epstein, A. G. MacDiamird, 141-150, Science and Application of conducting polymers, (Ed. W. R. Salaneck), Bristol: England (1991).
13. Conductive Electronic Polymers, (Ed. G. Gordon. Wallace, G. M. Spinks, P. R. Teasdale), Lancaster (1997).
14. E. Ehrenfreund, S. Vardeny, Phys. Rev. **B 36**, 1535 (1987).
15. J.P Pouget, M. E. Jozefowcz, Macromolecules **24**, 779 (1991).

Chapter 4

Charge transfer in Conducting Polymers

Some of the factors which can substantially influence the conductivity of CPs will be discussed in this chapter. By noting the contribution of each of these different factors, we will be able to determine the characteristics of charge transport in CPs. There are two basic mechanisms of single-particle transport in the solid state¹:

- i. *Band transport mechanism*: this is based on coherent diffusion: electrons move ballistically and are scattered by phonons and by disorder. This type of conduction is realized in metals with weak disorder or, in a more general case, for electronic states above the mobility edge¹. For a given degree of disorder, all states may either be localized or extended as a function of energy. The boundary separating these two regimes is called the mobility edge. The metal-insulator transition takes place when the electrons' Fermi energy crosses the mobility edge.
- ii. *Nonmetallic (phonon-assisted hopping) mechanism*: electrons jump between localized states by absorbing and emitting phonons. This hopping motion takes place for electrons with energies below the mobility edge¹.
- iii. *Reduction/oxidation (Redox) mechanism*: this is a charge exchange phenomenon most thought to contribute to the overall conductivity in either of case i or ii above. This redox mechanism is explained in more detail below².

Charge hopping among fixed polaron and bipolaron sites shall be considered as the primary charge-transport mechanism in the lightly doped EB systems. At high protonation levels, the polarons are arrayed to form a polaron lattice with metal-like transport within the partially filled polaron energy band³.

4.1 Charge exchange phenomena

Maximum conductivity is achieved when Pan is in the ES state, in this state the polaron states overlap to form mid-gap bands². The electrons are thermally promoted at ambient temperatures to the unfilled bands, which permit conduction. Because of the presence of structural defects, the occurrence of a charge exchange phenomenon, as depicted in figure 4.1, is thought to be necessary to produce the degree of conductivity obtained².

In CP hosts, electronic charge transport requires motion of charge both along the backbone and between chains to create a three-dimensional conducting matrix. In these materials, subtle variations in both the intra- and inter-chain organization can generate profound changes in the measured transport properties². Conductivity involves inter-chain or intra-chain proton exchange as well as electron transport. This explains the observed dependence of conductivity on the ambient humidity, as the presence of water in the polymer lattice would facilitate this proton-exchange phenomenon². This inter-chain charge hopping is represented in figure 4.1.

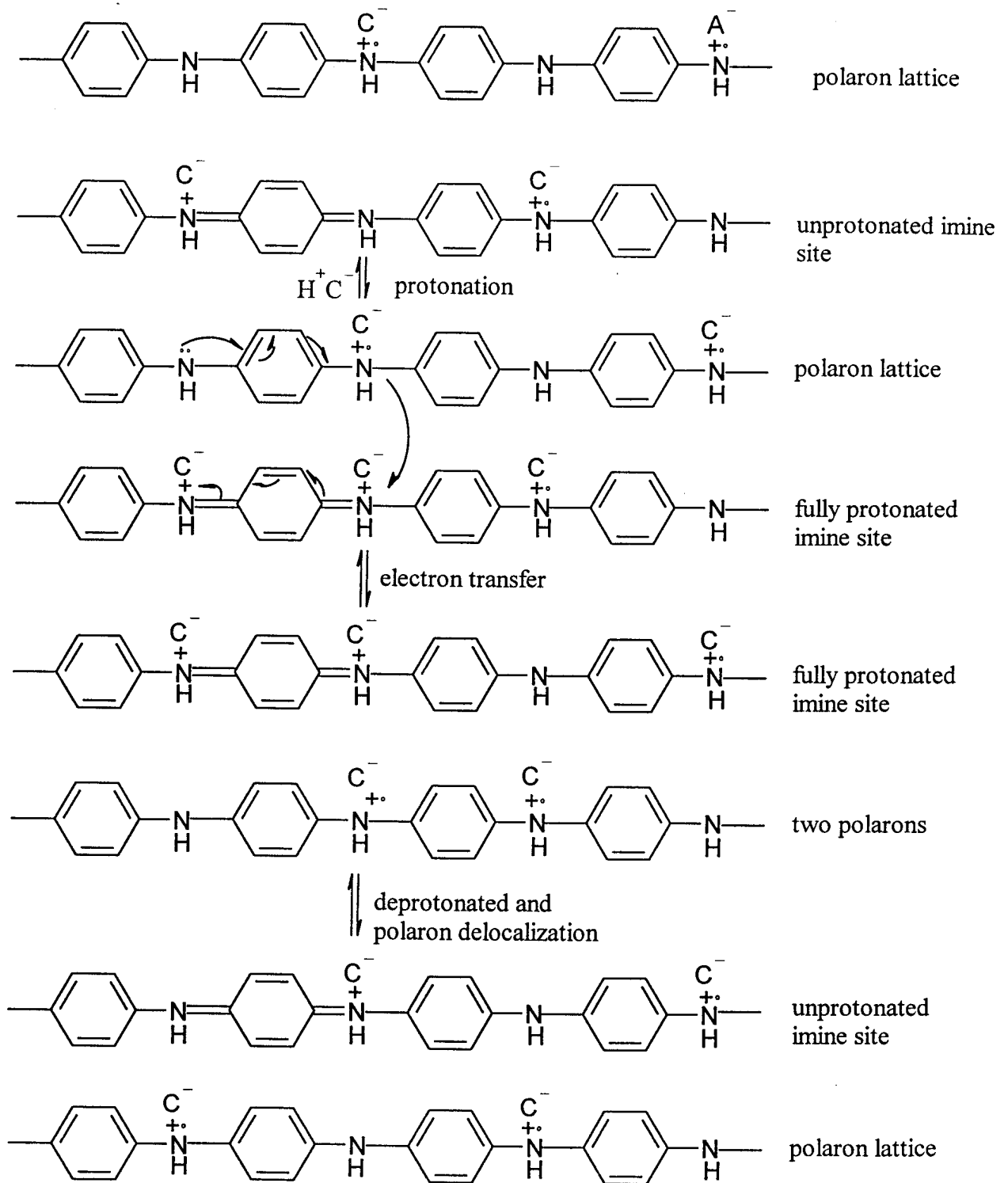


Figure (4.1): The inter-chain charge hopping mechanism for Pan^2 .

4.2 Factors affecting electrical conductivity

In CPs, electrical conductivity is dependent upon temperature, humidity, functional groups on the polymer and counter-ion species including the solvent it is cast from. In addition, the conductivity depends on preparation conditions, as they relate to the formation of structural defects and polymer morphology⁴.

4.2.1 Moisture content

The presence of moisture in Pan doped with HCl can increase the conductivity and significantly affects the other electronic properties. Figure 4.2 and 4.3^{2, 5-9} show the effect of humidity on conductivity and the role of moisture in the polymer's conductivity, respectively. While some water molecules are tightly bound, others are found to be relatively free and mobile⁹ The resulting increase in conductivity has been argued to be due to reduced potential barriers between the metallic islands⁹ An almost similar argument on the role of water in electrical conduction is that the presence of moisture in the polymer lattice facilitates the process of inter-chain or intra-chain proton exchange². The proton exchange takes place between the polymer solid phase and the water mobile phase¹⁰.

The temperature dependence of resistivity increases upon annealing of the Pan sample, indicating that the conduction mechanism has been affected. The conductivity of annealed samples can recover upon exposure to moisture⁸.

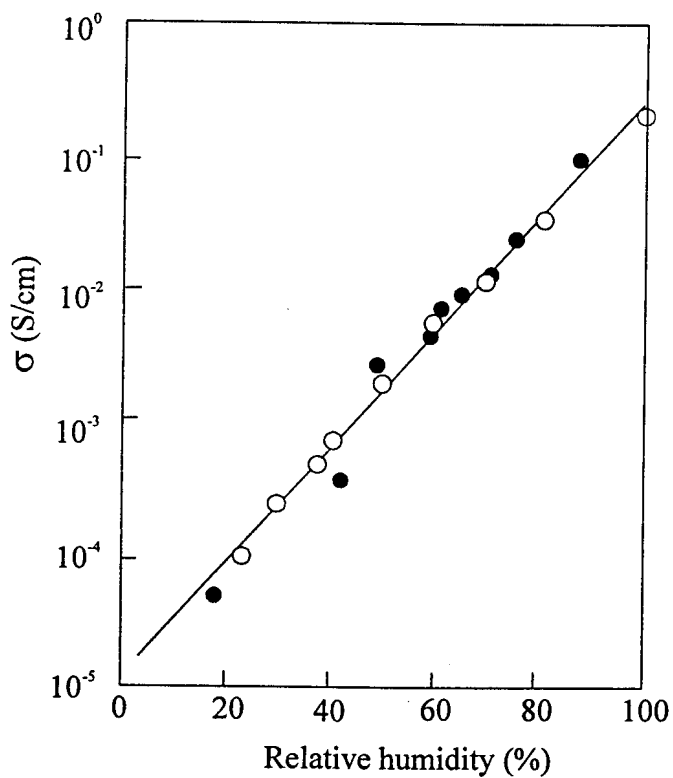


Fig (4.2): Relationship between the conductivity and relative humidity in the (○) desiccating and (●) moistening processes for a Pan-polyvinyl alcohol composite film¹⁰.

The mechanism by which the Pan film senses water molecules is shown in Figure 4.3, where “A” represents the dopant anion. At high humidity the doping of Pan is high and the polymer conducts. When water molecules are removed from the polymer, the dopant anions are de-doped in the acid form (HA) from the CP, resulting in a decrease in conductivity. This process is reversible and the conductivity changes with change in moisture¹⁰.

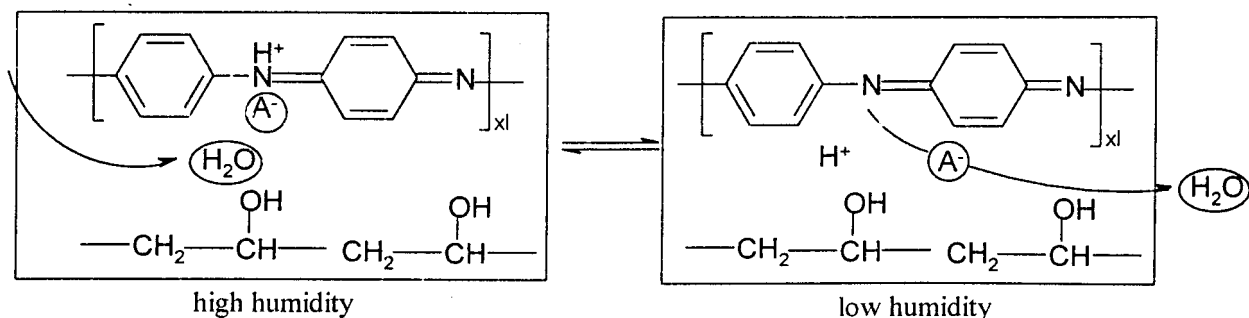


Fig (4.3): The role of moisture in the doping and de-doping of the polymer¹⁰.

4.2.2 Morphology and the heterogeneous media

The importance of morphology on conduction can be visualized from figures 4.4 and 4.5. The existence of defects or discontinuities in the extended conjugation (for example, cross link or ortho branch in the idealized head-to-tail chain of Pan and the attraction of the charge carriers to dopant counterions which pin them), localize the charge carriers¹¹.

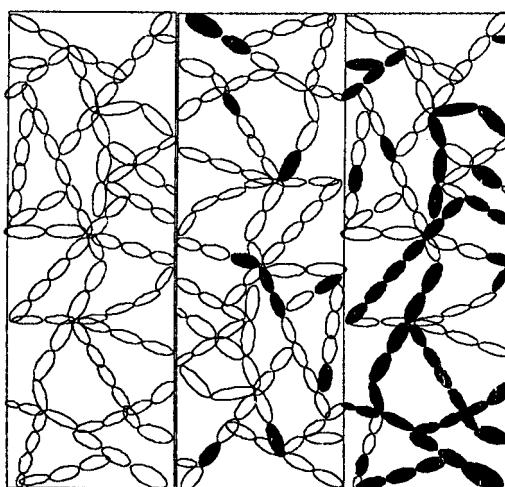


Fig (4.4): The relation of CP morphology to conduction. Doped segments (dark) in an interpenetrating structure, showing how increased doping finally provides a complete conduction pathway, left to right: undoped, partially doped (semiconducting) and partly doped (metallic) states¹¹.

It is perhaps more accurate to characterize the conduction process in CPs as the hopping of electrons between these charged carriers, a basis for the “hopping” models of conduction. CPs are considered as **disordered semiconductors** and, defects or breaks in the conjugation scatter electron transport¹¹. The inter-chain configuration of Pan in the base form (EB) significantly impacts the overall properties of the polymer¹¹.

The micrographs of CPs pellets and films demonstrate that the polymer solids consist of a heterogeneous structure of fibres and grains. An idealisation of this structure is shown in figure 4.5¹¹. Points 1 to 4 represent microprobes used to take electrical measurements. Probes 1 and 2 sit on the same chain and would permit direct conductivity – *intermolecular conduction*. Probes 2 and 3 would permit a hopping or tunneling process – *intermolecular hopping*. Probes 3 and 4 permit transport between fibres - *interfibrillar conduction*¹¹. In real experiments we measure transport between points 1 and 4 therefore we have a complicated superposition of various conduction processes. This superposition can be expressed as a series of resistances:

$$R_{1,4} = R_{1,2} + R_{2,3} + R_{3,4} \quad [4.1]$$

The largest resistance determines the material behavior. For lightly doped samples $R_{2,3}$ dominates and inter-polaron hopping takes place. In highly doped samples $R_{3,4}$ dominates. Hence hopping mechanisms are of paramount importance for charge transport in amorphous polymers¹¹.

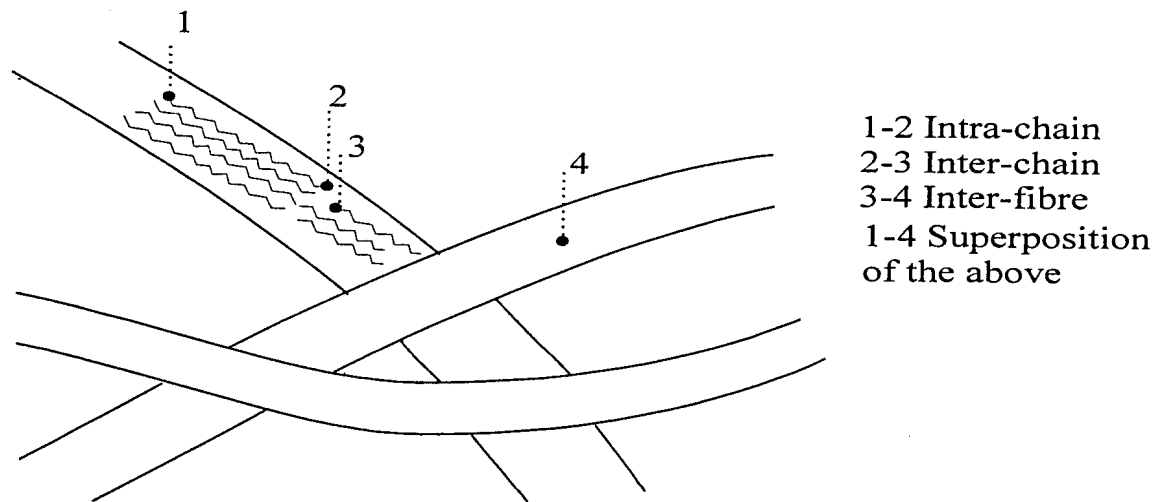


Fig (4.5): Schematic view of the fibrillar structure of a CPs¹¹.

Kaiser and Graham¹¹ have shown that the overall conductivity can be built up using standard expressions for different regions and they proposed a simple heterogeneous model as shown in figure 4.6.

Two key components of this model are:

- i. Temperature dependant conductivity is strongly influenced by thin barrier regions but is amplified by geometrical factors depending on the relative length of the highly conducting region (σ_1) to the total length¹².
- ii. The presence of a disordered metal region (σ_4) and phonon assisted transport in barrier regions (σ_3)¹².

The overall conductivity is expressed as in equation 4.2 where a , c , d , and q are the parameters including geometric factors. The first term ($a \exp(-[(h/2\pi)\omega_o]/k_B T)$) corresponds to conductivity in the metallic regions from Kivelson and Heeger, $(h/2\pi)\omega_o$ is the energy of the phonons that backscatter electrons and h is the Planck's constant.

$$\sigma^{-1} = a \exp(-[(h/2\pi)\omega_o]/k_B T) + \{c \exp[-(T_o/T)^{1/2}] + d + qT^{1/2}\}^{-1} \quad [4.2]$$

The first term in the bracket corresponds to the hopping/tunnelling mechanism from Sheng and Klafter¹¹. The remainder of the terms in the brackets ($\{c \exp[-T_0/T]^{1/2} + d + qT^{1/2}\}^{-1}$) comes from the electron-electron interaction in the disordered metal region, which occur parallel with the hopping/tunnelling region. In CP samples, contributions due to metallic regions are very small and the conductivity is mainly governed by the tunnelling/hopping process with a decreasing conductivity, presumably due to the lack of the metallic path in the barrier regions¹².

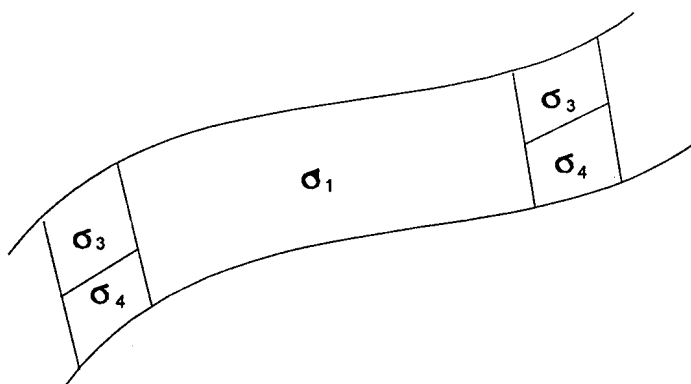


Fig (4.6): Conduction model in a fibril by Kaiser and Graham. Barriers consist of disordered regions in which hopping or tunneling occurs (σ_3) in parallel with a region showing metallic conductivity (σ_4). The larger regions in series with the barriers are metallic with high conductivity (σ_1)^{11,12}.

4.2.3 Impact of aggregation

Aggregates are formed in EB as a result of inter-chain interaction via hydrogen bonding between amine and imine sites. Reduction of the leucoemeraldine form eliminates the H-bonding and the aggregation⁷. The extent of aggregation on the polymer will impact on the solubility and solution characteristics of the polymer. The degree of aggregation on the polymer will depend on the conditions used to synthesize the polymer. Deaggregation facilitates a conformational change through chain expansion. Since doping results in a polar chain, the electrostatic repulsion of the ions on the doped chain also favors a chain expansion⁷.

4.2.4 Minor structural defects

Figure 4.7 (a) and (b) are micrographs of pellet and film surfaces for Pan doped with HCl respectively. Defects indicated from the surface profile, such as cracks in the material, have a direct effect of reducing conductivity. At the same time the volume of the conducting material imposes limitations on conductivity.

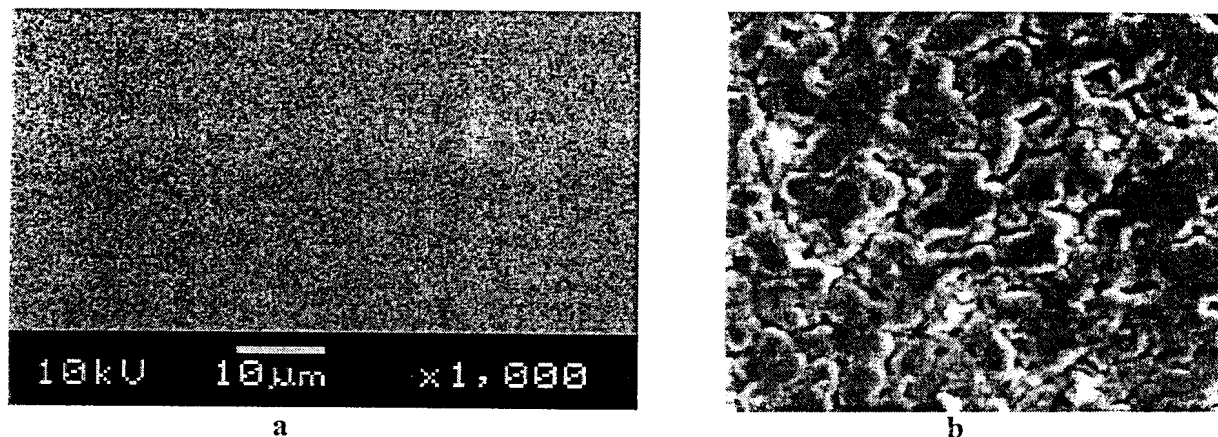


Fig (4.7): Surface SEM images for a doped Pan ES, film (a) and pellet (b), the pellet image was magnified at X 3,000.

4.2.5 Carrier mobility

The carrier mobility is the magnitude of the drift velocity per unit electric field. Carrier mobilities give an indication of the degree of perfection of the structural organization, purity and whether charge transport is due to hopping or band motion. Room temperature mobilities for CPs range from less than 10^{-7} to $\sim 0.5 \text{ cm}^2/\text{V}/\text{s}$, whereas they are typically 1350 and 3600 for n-type silicon and germanium, respectively. Mobilities depend on temperature as a modest power law.

For thermally activated charge transport, the mobility describing 3-dimensional hopping is obtained using the Einstein diffusion relation¹³.

$$\mu = \left(\frac{ea^2\omega}{6k_B T} \right) \exp\{-E_A / k_B T\} \quad [4.3]$$

where a is the hop distance (this distance is not the average chain separation but the average distance that carriers are able to travel along the chain between the thermally-activated inter-chain transfer processes), E_A and ω are the barrier to hopping (energy gap) and the average frequency of the optical phonons which modulate the chain dimerization, respectively. The mobility (μ), from the above equation can be increased through improving the structural order in the polymer and/or to move from the regime in which bipolaron hopping model applies to the metallic regime in which screening by other charges present removes the barrier to transport¹³.

4.2.6 Doping level

The conductivity of a CP increases with increasing doping across certain critical doping level ranges. The conductivity increase within a narrow applied potential range follows an exponential relation of the form¹¹:

$$\sigma(E) = \sigma_o \exp([E - E_o] / s) \quad [4.4]$$

Where σ_o is the conductivity at reference potential E_o , and s is the slope of $\log(I_s)$, (I_s is the steady state current at potential E) vs. E plot¹¹.

The variation of room temperature conductivity $\sigma_{(300K)}$ of ES as a function of dopant concentration (Cl/N)% is shown in figure 4.8. The conductivity of the sample gradually increases with an increase of dopant concentration. At high doping levels, the resistance between the fibres, $R_{3,4}$, dominates (figure 4.5) and the model of fluctuation-induced tunneling should be applicable¹¹. This model assumes elastic tunneling at low temperatures and at high temperature, an activated process is added⁸.

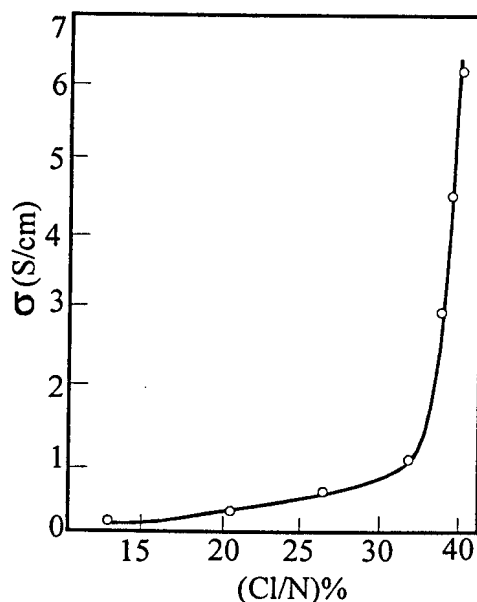


Fig (4.8): Variation of conductivity of ES with dopant concentration at 300 K⁶.

For DC conductivity this should be variable range hopping, hopping between localized electronic states, which are distributed at random in space and energy¹¹.

4.2.6.1 50% doping

As shown in the previous chapter, (figure 3.3,) EB consists of amine (-NH-) and imine (=N-) sites in equal proportions^{2, 4}. The imine sites are protonated to give the bipolaron (dication salt). However, they dissociate to form the delocalized polaron lattice⁵, (figure 3.10). At doping levels higher than 50%, some amine sites are protonated. At doping levels lower than 50%, some imine sites remain unprotonated. In both instances, delocalization of the charge carriers over the polymer backbone is disrupted, thereby, reducing the polymer conductivity².

If a significant proportion of these unconducting phases occur, polyaniline behaves in a manner equivalent to a conducting system in which metallic islands are dispersed throughout a non-conducting media. In such a system, charge transport is through “charge energy-limited tunneling”, involving long-range hopping².

4.2.7 Temperature

The electrical properties of CPs are strongly dependent on the extent of disorder present in the material. The extent of disorder is characterized in terms of the temperature dependence of conductivity⁶. By considering the temperature range from near absolute zero, metals, semiconductors, disordered semiconductors and insulators have the following conductivity dependencies:

- A metal's DC conductivity increases slightly with decreasing temperature, and reaches a finite limiting value near absolute zero¹⁻⁵.
- A semiconductor's conductivity decreases with decreasing temperature and remains finite at temperatures below 50 K¹⁻⁵.
- Conductivity of a crystalline semiconductor vanishes exponentially approaching absolute zero, while disordered semiconductors vanishes slowly¹⁻⁵.
- An insulator's conductivity decreases with decreasing temperature and vanishes at temperature near absolute zero¹⁻⁵.

Figure 4.9 shows the conductivity/temperature relationship of Pan. The conductivity increases as the temperature increases from 30 K, implying a hopping charge transfer mechanism where as conductivity decreases with temperature for band transport. In order to explain such behavior, the DC data are presented in the light of several models: Arrhenious plot, CELT model, Kivelson model and Mott's VRH model¹³. A detailed explanation of the models is presented in the next chapter. Because of the weak temperature dependence of conductivity, charge transport is analyzed here as 3-dimensional among localized states as described by Mott for non-interacting carriers⁶ At high temperature, phonon scattering dominates impurity scattering. This destroys the elastic scattering interference responsible for electron localization and explains the observed high conductivity. With decreasing temperature the localization effects become strong, and this interplay between the disorder and the phonon scattering leads to the observable decrease in conductivity with temperature¹.

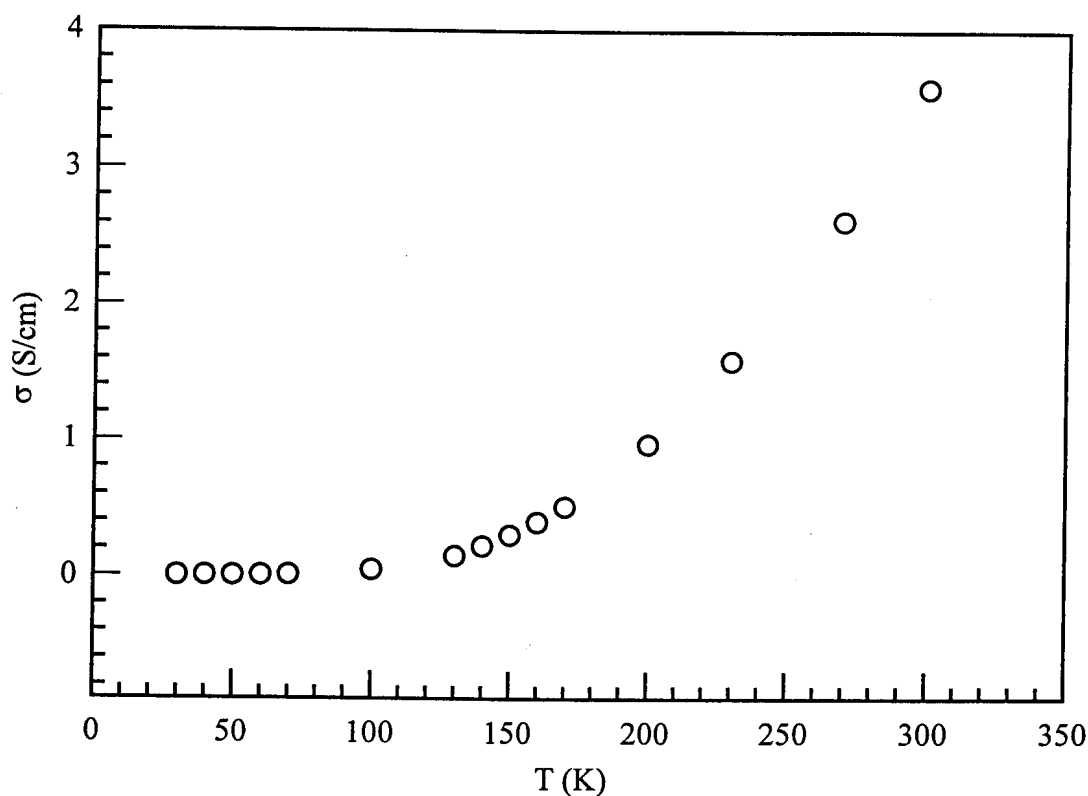


Fig (4.9): Variation of conductivity of Pan with temperature⁶

4.2.8 Conjugation length

A further property, which can influence conductivity, is the conjugation length, which can be defined as the extent of delocalization along the chain before a defect is encountered¹¹. Studies on CPs have indicated that the conductivity decreases with decreasing conjugation length¹¹. An increase in inter-molecular interaction results in an increased conductivity. It is noted in this respect that a short conjugation length is one of the key limiting factors for the conductivity of CP's. Hypothetical calculations have shown that conductivities up to 10^7 S/cm, far exceeding that of copper, could be obtained if one were truly able to synthesize a CP with extended conjugation along its entire chain¹¹.

4.2.9 Orientation and coherence length

One characteristic of highly conducting Pan is a high degree of orientation¹¹. Electrosynthesised polymers are produced with higher orientation, contributing to their higher conductivity compared to chemically synthesized material. Higher orientation results in more order, which seems to introduce the 3-D carrier transport¹². Crystallite size is represented by the coherence length (L_c) and is expressed as:

$$L_c = 0.9\lambda/B\cos\theta \quad [4.5]$$

where λ is the wavelength of the radiation, B is the reflection width of the half-height and θ is the Bragg angle¹².

4.2.10 Plasticizer

The addition of a plasticizer (for example: N-methylpyrrolidinone (NMP)) to the EB solution, results in highly crystalline EB films with no mechanical deformations. Crystallinity is due to the effect of deaggregation and the local mobility that the plasticizer provides which allows chains to crystallize. The solvent can solvate the individual chains and, thus a conformational change can occur in which chains become more expanded⁷.

4.2.11 Processing solvents and solutions

The solution characteristics determine the morphology of EB films derived from such solutions. EB films will have different levels of deaggregation and chain expansion, depending on the solvent from which they have been processed and therefore, will exhibit different properties⁷.

The amorphous phase exists in various conformations, such as “coil”, “expanded-coil” and “rod-like” conformation. These conformations are obtained depending on the

processing solution, for example, Pan processed from m-cresol and NMP/LiCl, has a more expanded coil type of conformation and exhibits higher conductivity than the same salts processed from solvents such as NMP⁷. Samples of the same chemical composition prepared from different solvents may have different local orders, thus very different conductivities¹⁵.

4.2.12 Dopant molecules

A dopant not only generates a charge carrier by chemical modification, but also provides intermolecular links and sets up a microfield pattern affecting charge transport. Any disturbance of the periodicity of the potential along the chain induces a localized energy state. Localization also arises in the neighborhood of the ionized dopant molecule due to the Coulomb field¹⁶.

4.2.13 Solution concentration and crystallinity

The crystallinity of EB films depends on the degree of aggregation in the polymer. Films cast from highly concentrated solutions, where the structure is more aggregate, are more amorphous compared to films cast from less concentrated solutions⁷.

4.2.14 Synthesis procedure

A comparison is made between electrochemical and chemical synthesis of Pan.

In **electrochemical synthesis**, different experimental conditions and/or dopant ions do not necessarily give identical results¹⁷. By varying the conditions, for example, Pan (BF_4^- doped) film grown on a platinum electrode at a constant potential of $0.7 V$ (vs. saturated calomel electrode (SCE)) for *16 hours* was observed to have a compact microspheroid morphology, whereas a film (ClO_4^-) doped and grown on indium tin oxide (ITO) at a constant current of $50 \mu A$ for *90 minutes* had a highly fibrillar morphology on a micropsherooid underlayer of the polymer¹⁵. The final oxidation state of Pan produced

during electrochemical synthesis can vary greatly depending on preparation conditions (the different oxidation states of Pan).

In **chemical synthesis**, it is possible to obtain a polymer of varying: molecular weight distribution, polydispersity index (chain length), morphology and oxidation states. These variables impact on the polymer conductivity and device shelf life¹⁷.

4.2.15 Stretching

The conductivity of a CP increases steeply with increasing draw ratio l/l_o , where l is the length after drawing and l_o is the original length before drawing (figure 4.10). The initial stretching results in higher orientation and denser packing in fibrillar structure but additional stretching causes sliding of different fibrils against each other and finally small cracks develop¹². X-ray diffraction studies of EB subjected to increasing draw ratio l/l_o show an increase in crystallinity (see figure 4.11). The draw ratio, crystallinity and conductivity data show that the conductivity of fibers increases monotonically with increases in apparent crystallinity¹⁸.

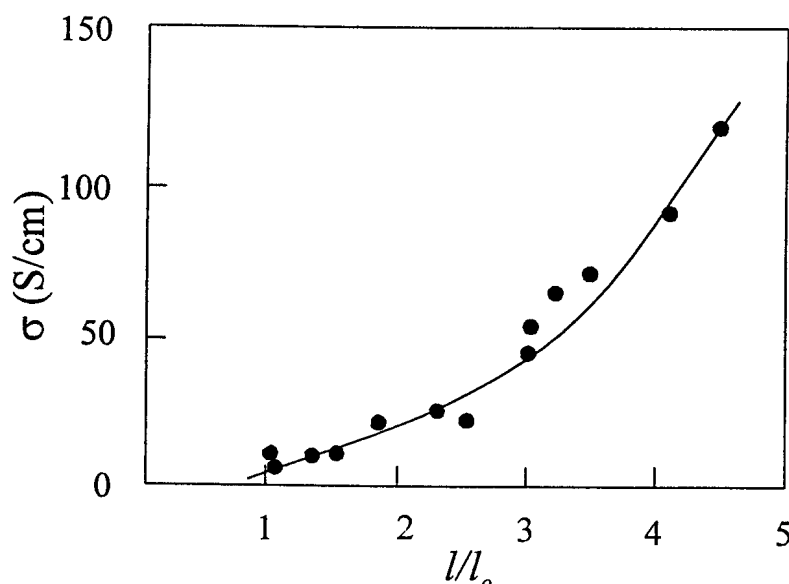


Fig (4.10): Conductivity of the HCl-doped drawn fibers as a function of increasing draw ratio l/l_o ¹⁸.

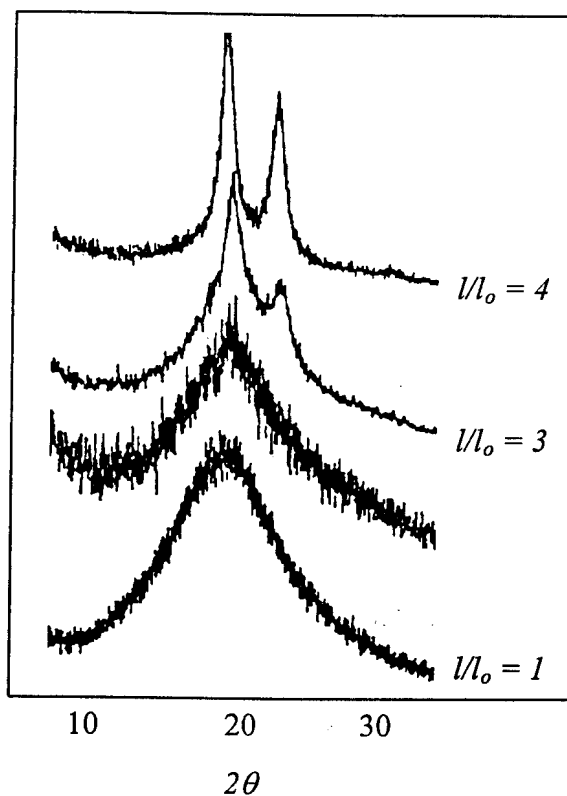


Fig (4.11): X-ray diffraction spectra of ribbons of EB of increasing draw ratio l/l_0 ¹⁸.

4.2.16 Molecular weight

In figure 4.12 it can be seen that the conductivity of a doped (1M HCl) ES rises monotonically with molecular weight (Mw) up to a value of 150 000 (~1.600 ring-nitrogen repeat units), after which it changes relatively little. However, samples with different molecular weights, and therefore different conductivities, exhibit approximately the same crystallinity as determined by X-ray diffraction studies¹⁸.

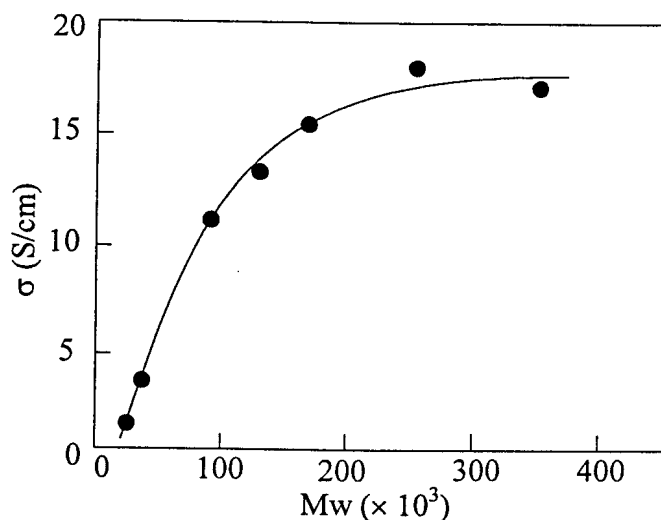


Fig (4.12): Dependence of conductivity of ES on molecular weight¹⁸.

4.3 The metallic behavior of polyaniline

In general, the conductivity of Pan can be said to depend on the inter-link of metallic regions with insulating regions. An abundance of metallic regions results in the following metallic characteristics displayed by heavily doped CPs:

- Relatively high conductivity: 200 S/cm for doped Pan pellets, Pan-CSA (camphor sulphonic acid) has a room temperature conductivity of 200-400 S/cm, comparable to Mott's minimum metallic conductivity^{19,20}.
- Pauli temperature independent magnetic susceptibility²⁰.
- Linear term in the specific heat capacity²⁰.
- Absorption throughout the infrared region with no energy gap²⁰.

However, these metallic features in the bulk transport, are severely limited by strong disorder. The polymers cannot display the following traditional signatures of metallic transport:

- Resistivity (ρ) with a positive temperature coefficient, $d\rho/dT > 0$;
- Thermoelectric power (S) proportional to temperature²⁰.



Disorder results in the localization of states. If the magnitude of the disorder potential is large compared with the bandwidth, all states become localized and the system will be an insulator. In such a state, there is no energy gap. Consequently, the insulating property results since the Fermi level (E_F) lies in an energy interval in which all states are localized – the system is a Fermi glass. In such a system, the conductivity is temperature activated. At high temperatures, the activation energy is a measure of the energy difference between E_F (which lies in the region of localized states) and the mobility edge. At lower temperatures, variable range hopping (VRH) transport results from the existence of unoccupied localized electronic states near E_F ²⁰.

References

1. J. Joo, V. Prigodin, A. G. MacDiarmid, A. J. Epstein, *Phys. Rev. B* **50**, 12226 (1994).
2. *Conductive Electroactive Polymers*, (Ed. G. Wallace, G. M. Spinks, P. R. Teasdale), Lancaster (1997).
3. J. Ginder, A. J. Epstein, *Phys. Rev. B* **41**, 10674 (1990).
4. K. Lee, A. J. Heeger, *Phys. Rev. B* **20**, 14884 (1993).
5. M. E. Jozefowicz, A. J. Epstein, A. G. MacDiarmid, *Phys. Rev. B* **39**, 12958 (1989).
6. M. Gosh, A. Barman, S. K. De, Chatterjee, *J. Appl. Phys.* **84**, 806 (1998).
7. M. Angelopoulos, R. Dietro, W. Zheng, A. G. MacDiarmid, A. J. Epstein, *Synth. Met.* **84**, 35 (1997).
8. N. J. Pinto, P. K. Kahol, B. J. McCormick, *Phys. Rev. B* **53**, 10690 (1996).
9. A. Atushi, H. Ishikawa, K. Amano, M. Satoh, *J. Appl. Phys.* **74**, 296 (1993).
10. K. Ogura, T. Saino, H. Shiigi, *J. Mater. Chem.* **7**, 2363 (1997).
11. *Conducting Polymers, Fundamentals and Applications*, (Ed. P. Chandrasekhar), Kluwer academic publishers: Boston (1999).
12. J. Tsukamoto, *Adv. in Phys.* **41**, 509 (1992).
13. R. H. Friend, J. H. Burroughes, K.E Ziemelis, *Science and Application of conducting polymers*, (Ed. W. R. Salaneck), Bristol: England (1991).
14. M. Gosh, A. Barman, A. K. Meikap, S. Chatterjee, *Phys. Lett. A* **260**, 138 (1999).
15. A. J. Epstein, *MRS Bulletin* **22**, 16 (1997).
16. A. G. MacDiarmid, W. Zheng, *MRS Bulletin* **22**, 24 (1997).
17. D. C. Trivedi, *Handbook. of Organic Conductive Molecules and Polymers 2* (Ed. H. S Nalwa), John Wiley and sons: New York (1997).
18. A. G. MacDiarmid, A. J. Epstein, *Science and Application of conducting polymers*, (Ed. W. R. Salaneck), Bristol: England (1991).
19. R. Pelster, B. Wessling, *Phys. Rev. B* **49**, 12 718 (1994).
20. R. Menon, A. J. Heeger, Y. Cao, *Phys. Rev. B* **48**, 17 685 (1993).

Chapter 5

Characterization of Polyaniline

One of the aims of this study has been to clarify the transport mechanisms in CPs. To this end, different characterization methods have been employed for the characterization of CPs. The mechanisms behind charge transfer in CPs is still under debate and we have employed different methods during this work in order to try and narrow down possible mechanisms. Electrical characterization provides an excellent and very sensitive way to determine the electrical characteristics of CPs. In the present study the following techniques were used in assessing and explaining electrical properties of such materials:

- Scanning electron microscopy (SEM) for morphology analysis,
- Fourier transform infrared spectroscopy (FTIR) for molecular level analysis,
- Differential scanning calorimetry (DSC) and thermal gravimetry analysis (TGA) for analysis of decomposition behavior and crystallinity.
- Temperature dependant current – voltage (I-V) measurements.

From the various experimental results such as conductivity, magnetic susceptibility and spin dynamic measurements, it seems that doped Pan segregates into either granular 3-d metallic islands surrounded by amorphous regions or an isolated conducting chain in an insulating polymer matrix¹. However, conductivity in Pan shall be analyzed in terms of the models summarised in table 5.1, these models shall be described in more detail in section 5.8.

Table 5.1: Summary of conduction models

<i>Model</i>	<i>Area of application</i>
Mott's Variable Range Hopping (VRH) ¹ ($\ln\sigma$ vs. $T^{-0.25}$)	<ul style="list-style-type: none"> - Disordered semiconductors, including CPs - Temperatures above 30K, being also dependant on the dimensionality of charge transfer process
Arrhenius plot ² ($\ln\sigma$ vs. T^{-1})	<ul style="list-style-type: none"> - Temperatures above 250 K for most Pan samples
Kivelson ² ($\ln\sigma$ vs. $\ln T$)	<ul style="list-style-type: none"> - Highly doped Pan samples
Activation energy ² ($\ln\sigma$ vs. $T^{-0.5}$)	<ul style="list-style-type: none"> - Temperatures above 280 K - Over a wide doping level range - Assumes conduction is attributed to electron hopping
Sheng ² ($\ln\sigma$ vs. $T^{-0.5}$)	<ul style="list-style-type: none"> - Assumes a system of metallic particles embedded in a dielectric matrix - Highly doped Pan (about 50%), ratio of dopant ions per monomer units

5.1 Current-voltage measurements at ambient temperatures

Current-voltage measurements were first made to ensure that no significant contribution to conductivity occurred due to ionic conduction; this was achieved by passing a constant current through a sample and monitoring the potential difference as a function of time. If an ion contribution to conductivity occurred, it would have been manifested as a decrease in the sample conductivity as the number of ions were depleted. Since this did not occur it was assumed that conduction was occurring in all samples by an electronic mechanism. Current-voltage characteristics were found to be ohmic in all samples in the current range 5nA to 5 μ A.

5.1.1 Ohmic contacts

The electrical properties of Pan were measured using the four-point probe and the Montgomery techniques. These two methods are based on point-electrodes and thus assume a spherical symmetry of the electric field, meaning that they are not really applicable to strongly inhomogeneous materials. For both methods the measurement of conductivity relies on passing a stabilized current through the sample and measuring the voltage drop at the voltage electrodes. The simplest device structure is a bar of the polymer with two electrodes connected via ohmic contacts. The conductivity (σ) of a bar of p -type material is given by³

$$\sigma = e\mu_p p \quad [5.1]$$

where e is the electronic charge, μ_p the (hole) mobility and p the hole density. Because both the *free-carrier density* p and the *mobility* μ_p are functions of temperature, the conductivity is strongly temperature dependent³. The hole density is given as

$$p = 2^{\frac{1}{2}} (N_A N_V)^{\frac{1}{2}} \exp(-E_A / k_B T) \approx T^{\frac{3}{4}} \exp(-E_A / k_B T) \quad [5.2]$$

Here N_A is the acceptor concentration, N_V the density of states at the top of the valence band, E_A the activation energy of the acceptor, k_B the Boltzmann constant and T the temperature. The hole mobility depends on the limiting mechanisms described in chapter 4. The following models are equally possible:

$$\text{Acoustic phonons: } \mu_p \sim m^{*-5/2} T^{-3/2} \quad [5.3]$$

$$\text{Ionized impurities: } \mu_p \sim m^{*-1/2} T^{3/2} \quad [5.4]$$

$$\text{Optical phonons: } \mu_p \sim m^{*-3/2} T^{1/2} \quad [5.5]$$

In principle, we determine the activation energy for bulk conduction through the measurement of the conductivity as a function of temperature. In this model, the resistivity of the sample does not depend on the voltage.

5.1.2 Conductivity in the bulk samples

As stated in the previous chapters, several charge carriers contribute to the overall conductivity of the polymer, many structural imperfections are present in all polymers and thus, when discussing mechanism of bulk conductivity, these defects need to be considered. Conductivity is not only a result of charge transfer along the chain, but is also due to electron hopping between chains and between different conjugated segments of the same chain. In addition to these effects which act at a molecular level, bulk conductivity values are also dominated by electron transfer between grain boundaries and variations in morphology³. Thus the bulk conductivity (σ) can be represented by²:

$$\sigma = \sum \frac{n_i Z_i e v_i}{E} \quad [5.6]$$

Where,

n_i = number of charges carried by each type

Z_i = carrier type

e = electronic charge

v_i = drift velocity of an electron

E = electric field strength.

Equation 5.6 takes into account different charge carrier types, which contribute to the overall observed conductivity in the bulk polymer².

5.2 Four-point probe measurements

Considering a collinear four-probe array as in figure 5.1, current (I) is applied by two outer points and the voltage (V) is measured between two inner probes. For a semi-infinite sheet with thickness ($d \gg s$), where s is the separation between probes^{4,5}:

$$\sigma = I / 2\pi s V \quad [5.7]$$

This method was applied in measuring the current-voltage characteristics of Pan pellets.

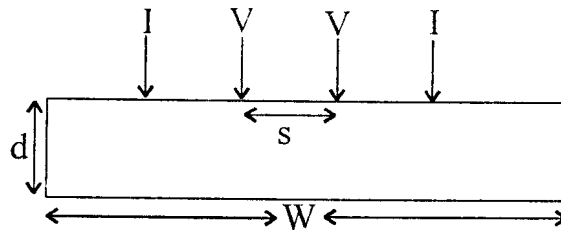


Fig (5.1): Outer electrodes on Pan pellet are current (I) electrodes while inner electrodes are voltage electrodes (V).

5.3 Montgomery method

This method was used in the measurement of the conductivity of thin films. Point electrodes are attached at the four corners of a square thin film, (fig. 5.2) and resistivity ρ , is given as⁵:

$$\rho = HER \quad [5.8]$$

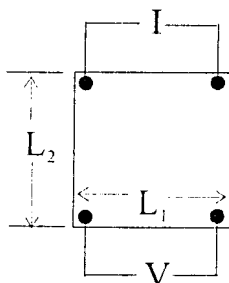


Fig (5.2): Current and voltage electrodes are attached to the four corners of the square sample (film/pellet)

Where H is a function of L_2/L_1 as shown in Table 5.1. R is the ratio of measured voltage to current (V/I). E is an effective thickness, which is equal to the actual thickness L_3 when $L_3 \ll (L_1 L_2)^{1/2}$, but never gets much greater than $(L_1 L_2)^{1/2}$. In the present study, L_1 was made equal to L_2 and therefore $H \sim 4.531$ according to table 5.2⁶. The average for L_3 for our films was about $50 \mu m$, while L_1 and L_2 were about 0.4 cm respectively.

Table 5.2. Selected values of the function H ⁶

L_1/L_2	0.25	0.5	0.6667	1.0	1.5	2.0	4.0
H	0.3207	0.8911	1.562	4.531	21.86	105.1	56 300.0

5.4 Conductivity measurements at $T > 300 \text{ K}$

Pellets of emeraldine salt (ES) were subjected to temperatures between 300 and 450 K at atmospheric pressure. The current-voltage characteristics were determined using the four-point probe method described above. The results from these relatively high temperature measurements were related to thermogravimetry results and the effect of moisture loss on conductivity was determined.

5.5 Conductivity measurements at $T < 300 \text{ K}$

These investigations were performed to verify which of the conduction models studied, best describes electrical conduction in Pan. Current-voltage measurements of Pan samples were taken and conductivity was calculated using the Montgomery and four-point probe methods. The intrinsic metallic state and also its dimensionality can be detected from the low temperature conductivity values. In the present work, we made an extensive study on the transport properties at low temperatures¹.

5.6 Measurement of the extent of disorder in a polymer

The extent of disorder in the polymer is characterized in terms of the resistivity ratio (ρ_r). The higher this value the more disorder is present in the material. ρ_r is described by the relationship:

$$\rho_r = \rho_{T(K)} / \rho_{300K} \quad [5.9]$$

Where $\rho_{T(K)}$ represents the resistivity at a temperature between 30 and 300 K⁷.

5.7 The metal -insulator transition

Menon *et al*¹ describes the metal-insulator (M-I) transition behavior in Pan depending on the ratio values (ρ_r). Three types of behavior are identified:

- i. metallic region ($\rho_r < 2$)
- ii. critical region ($2 < \rho_r < 6$)
- iii. insulating region ($\rho_r > 6$),

$$\text{for } \rho_r = \rho_{30(K)} / \rho_{300(K)} \quad [5.10]$$

5.8 Conduction models

A model of best fit is deduced from the measurement of the deviation of the experimental results from linearity when we plot curves of the variation of conductivity as a function of temperature for the models stated in the following section. While these and many other models have been proposed for conduction in CP, conduction remains a complex phenomenon, and to date no single model is comprehensively accurate. In varying degrees, the various models are able to account for the conduction behavior within a specific temperature range or doping range or dopant type, but then fail for other CPs. In one case, a 3-dimensional conduction model may be indicated, whereas in another case, it is not⁸.

5.8.1 The Mott – Variable Range hopping (VRH) model

The lack of ordering in CPs produces localized electronic states (polarons, bipolarons and solitons). The model of VRH assumes that localization is not very strong and differs at different locations within a material and thus postulates that conduction occurs by variable range hopping of electrons between these localized states. This electron hopping is assisted by phonons and sometimes depends on the initial and final energies (overlap of wave functions) of the states between which hopping occurs¹.

Mott's model is applicable to 1-, 2- and 3- dimensional conduction. However, since the one-dimensional model arises due to strong interchain coupling between bundles, the one-dimension conduction fails if all bundles are coupled.

Due to the weaker resistivity–temperature dependence, the model such as metallic islands arising due to large inhomogeneity and strong disorder is not valid for our samples. Our experimental results were analyzed according to 3-D conduction among localized states¹. The magnitude of the hopping conductivity is expected to be much less than that of Mott's minimum metallic conductivity (200 – 400 S/cm), while the conductivity of metallic states above the mobility edge remains higher than this boundary value⁸. In the

argument developed by Mott, conductivity as a function of temperature for three-dimensional hopping is given by:

$$\sigma(T) = \sigma_o \exp(T_o / T)^{1/(n+1)} \quad [5.11]$$

Where, n = dimensionality of the material's conductivity, σ_o is the room temperature conductivity⁹.

From the values of the fitting parameters σ_o and T_o , we can calculate the values of the density of states, $N_{(EF)}$, and average hopping distance R , from the following equations:

$$T_o = 24 / [\pi L_{loc}^3 k_B N_{(EF)}] \quad [5.12]$$

$$\sigma_o = (3/4) e^2 \gamma_o R N_{(EF)} \quad [5.13]$$

$$R = [3 L_{loc} / \{2 \pi N_{(EF)} k_B T\}^{1/4}] \quad [5.14]$$

Where k_B is the Boltzman constant and L_{loc} the localization length (localization length is the range in which a charge carrier in the CP can move without encountering a barrier) which is determined from the magnetic field dependence of conductivity data. L_{loc} (Å) was assumed to be 72 Å, after the work of M. Gosh *et al*¹. Temperature dependence should change with pressure, because the density of states at the Fermi level changes⁹.

A condition for application of the hopping theory is that: $R \gg L_{loc}^2$

5.8.2 The conductivity Arrhenius plot

Conductivity follows the Arrhenius behavior at temperatures above 250 K for most Pan samples.

$$\sigma = \sigma_e \exp(|E_F - E_C| / k_B T) \quad [5.15]$$

$E_F - E_c$ (activation energy) is the energy difference between the Fermi energy (E_F) and the mobility edge (E_c) and σ_e is the conductivity at the mobility edge².

5.8.3 Activated energy model

This model directly follows from Mott's model described above for conduction in 2-D. At lower temperatures, where the Arrhenius law fails, conduction is satisfactorily represented by the expression 5.16 for thermally activated conductivity².

$$\sigma = \sigma_o \exp(-\sqrt{T_o / T}) \quad [5.16]$$

Where T_o and σ_o are described by equation 5.12 and 5.13 respectively.

Conduction is attributed to electron hopping, the origin and size of electronic localization centers and barriers have not yet been identified¹¹. The hopping activation energy decreases as conductivity increases, as would be expected for higher state densities, since the conductivity increases as the hopping sites get closer together.

5.8.4 Kivelson model

This model represents the conductivity of lightly doped Pan samples. The conductivity follows the power law²:

$$\sigma(T) \propto T^n \quad [5.17]$$

where, $n > 10$.

In Kivelson's model, there should be the same temperature dependence at all pressures⁹.

5.8.5 Sheng's model

This model applies mostly to highly doped polymers. It assumes conduction between the “metallic islands” within the polymer and yields the following temperature relation:

$$\sigma = \sigma_o \exp(-T_1 / (T + T_o)) \quad [5.18]$$

Where T_o is described by equation 5.12. T_1 is an additional fitting parameter, and the fitting parameters are dependant upon the properties of the potential barriers (insulating islands or interfibrillar spaces) between the highly conducting islands⁸. The charge transport is thought to result from tunneling induced by thermal fluctuations. The above equation predicts conductivity monotonically decreasing with temperature but still yielding a finite value at near absolute zero (due to quantum mechanical tunneling) and a saturation value of conductivity at higher temperatures. Several variations of Sheng 's model exist³.

Each of all the above models are but one part of the whole truth, being valid under different ranges and conditions of doping, temperature and other variables.

5.9 Polymer sample morphology

The morphology of the polymer has an effect on the electrical conductivity of the material. As shown in the previous chapter, amorphous regions disturb conduction through band to band hopping allowing only fiber to fiber hopping conduction which is more unlikely and thus we end up with low conduction material and very low charge mobility. Transport in the crystalline regions is metallic like and the magnitude of conductivity is higher. Charge mobility is also high. A 50% crystalline polymer is more conductive as compared to a 20% crystalline polymer. The following techniques were used to analyze polymer morphologies.

5.9.1 Scanning electron microscopy (SEM)

Polymer structure and morphology are greatly affected by synthesis conditions such as electrode materials for electrosynthesis, solvent and electrolyte salts, oxygen and water content of the system and the current density used for electropolymerization. SEM is used for the analysis of polymer samples in the film and pellet form. Films appear generally smooth, while pellets show uneven surfaces and the possible existence of macroscopic defects such as cracks (see chapter 8 figure 8.4).

5.10 Fourier-Transform-Infrared (FTIR) and Raman spectroscopy

The vibrational frequencies of a molecule can be determined by infrared spectroscopy and Raman spectroscopy. Both techniques depend on the interaction of electromagnetic radiation with matter, but the physical causes are different. In many molecules it is therefore possible to observe vibrations of different symmetry by different spectroscopic techniques.

- i. Raman spectroscopy was used initially for the analysis of the changes in the molecular structure of Pan as result of the annealing.
- ii. Infrared spectroscopy was used to evaluate the effect of annealing on the molecular structure of emeraldine base and emeraldine salt, as well as to compare the Pan we synthesized in our laboratory with commercially available Aldrich Pan in their doped and undoped forms.

FTIR spectroscopy is commonly used to study organic compounds as it provides information about:

- i. the presence or absence of certain functional groups in a molecule
- ii. the extent of hydrogen bonding (intra- and inter molecular hydrogen bonding)
- iii. conformational orientation of molecules

The theoretical basis of FTIR spectroscopy can be explained in the following way:

5.10.1 Molecular vibrations

A polyatomic molecule possesses several vibrations and these may be infrared active or inactive according to the symmetry of the vibrational mode. The energy of these vibrations corresponds to that of the infrared region. Therefore, absorption of infrared radiation of the appropriate wavelength results in a vibrationally excited state. Infrared radiation is absorbed if the frequency of the radiation matches that of an allowed vibrational transition. The bond(s) undergoing the vibrational transition must have a dipole moment and the absorption of radiation must result in a change of that dipole moment, that is, vibrations in a molecule must give rise to an unsymmetrical charge distribution. The greater the change in the dipole moment, the more intense the absorption. The vibrations of homonuclear diatomic molecules (e.g. O₂, N₂, etc.) do not result in infrared absorption and therefore we apply Raman spectroscopy in which light is scattered rather than absorbed.

5.10.2 Types of oscillations

Molecules can undergo different types of oscillations and thus may absorb energy at more than one wavelength. During vibration, the molecule's bonds stretch, contract and bend so that the structure oscillates around the most stable configuration.

(a) Stretching vibrations (b_{u1} and b_{u3}).

Stretching vibrations can be symmetric (b_{u1}), i.e. expansion and contraction of the molecular bonds occur in phase or asymmetric (b_{u3}), formed by combining the expansion of one bond with the contraction of the other, i.e. out of phase.

This symmetric and antisymmetric combination occurs in all cases where two bonds are equivalent due to molecular symmetry.

(b) Bending vibrations (b_{u2})

Bending vibrations can be relatively complicated motions such as scissoring, rocking, wagging or twisting. An infrared spectrometer measures the frequencies of the infrared radiation, which have been absorbed by a given sample. Most FTIR spectra are complex because of the overtones and coupling peaks.

5.10.3 Infrared spectra of polyaniline as from the work of Epstein *et al*¹²

Results from chapter 8, show that the peak positions vary to a low degree, depending on whether the Pan was obtained from electrosynthesis, doped in HCL or Aldrich Pan (camphor sulfonic acid doped). The spectral shifts/changes are taken as adequate indicators of molecular changes in the polymer.

- i. EB spectrum shows strong absorption at 827, 1150, 1320, 1501, and 1591 cm^{-1} .
- ii. Upon protonation of EB to ES the existing features show an increase in the oscillator strength and the bands at 1501 and 1591 cm^{-1} show a red shift to 1486 and 1568 cm^{-1} respectively. No new band appears upon doping.
- iii. p-doping of LEB with HCl to ES results in a significant change of the spectra, a new band is seen at 1150 cm^{-1} and the bands at 1500 and 1591 cm^{-1} change intensity and /or shift. Several of these features are observed for EB as it changes to ES.
- iv. The 1591 cm^{-1} band for EB is consistent with the presence of quinoids in this material.
- v. The infrared spectra of EB is described in terms of *para*-disubstituted benzene and additional modes are associated with symmetry breaking of the benzeoids due to the presence of quinoid groups.
- vi. The band at 816 cm^{-1} for LEB is assigned to a b_{u2} C-H out-of-plane deformation of the benzoid groups. The band at 1284 cm^{-1} for LEB is due to b_{u3} benzenoid-amine stretching vibration. The intense band at 1497 cm^{-1} is for b_{u3} C-C ring-

stretching mode; the relatively weak one at 1613cm^{-1} is likely to arise from the disorder-induced b_{u1} C-C ring stretching mode.

- vii. For EB, two new bands are present at 1150 and 1591 cm^{-1} corresponding to two strong Raman bands of LEB at 1188 and 1623 cm^{-1} respectively. The 1166 cm^{-1} mode is assigned as either a b_{u1} C-H in-plane ring deformation or a b_{u1} ring-amine stretching vibration. The 1591 cm^{-1} mode has two contributions: C-C ring stretching vibration of the quinoid groups and b_{u1} C-C ring stretching mode of the benzenoid groups (as in LEB, but much stronger). Again the symmetry-breaking role of the quinoid groups present in EB causes the Raman mode to become infrared active¹².

The relative intensity of the two bands at 1150 and 1591 cm^{-1} can be used as a measure of the oxidation state (i.e. the number of quinoid groups) in Pan between LEB ($1-y = 0$) and PNB ($1-y = 1$). The monotonic increase in the intensity of the 1590 cm^{-1} absorbency is taken as indicating the continued growth in the number of quinoid-like rings in the polymer chain¹³. Doping of ES results in an overlap of the infrared bands with the electronic continuum of the polaron band. The resulting absorption can be described in terms of a Fano effect causing shifts and large enhancement of the infrared bands¹².

Reference:

1. M. Gosh, A. Barman, S. K. De, S. Chatterjee, *J. App. Phys* **84**, 806 (1998).
2. M. Gosh, A. Barman, S. K. De, S. Chatterjee, *Phys. Let. A* **260**, 138 (1999).
3. <http://www.sci.port.ac.uk/aeg/jrsmith/chapter1.htm>
4. W. Pukacki, *Mat. Sc. Forum* **122**, 255 (1993).
5. S. M. Sze, *Physics of semiconductor devices*, (Ed. S. M. Sze), New York (1981).
6. H. C. Montgomery, *J. App. Phys.* **42**, 2971 (1971).
7. M. Gosh, A. Barman, S. K. De, S. Chatterjee, *J. App. Phys.* **84**, 806 (1998).
8. *Conducting Polymers, Fundamentals and Applications*, (Ed. P. Chandrasekhar), Kluwer academic publishers: Boston (1999).
9. J. Joo, V. N. Prigodin, A. J. Epstein, *Phys. Rev. B* **50**, 12226 (1994).
10. S. Curran, *Handbook of Conductive Molecules and Polymers 2* (Ed. H. S Nalwa), John Wiley and sons: New York 25 (1997).
11. R. Pelster, V. B. Wessling, *Phys. Rev. B* **49**, 12718 (1994).
12. http://lifshitz.physics.wisc.edu/www/rguest/re_winokur_over.htm
13. A. J. Epstein, R. P. McCall, J. M. Ginder and A. G. MacDiarmid; *Spectroscopy of advanced Materials*, (Ed. R. J. H. Clark), Chichester, Wiley (1991).